

1 **Supplemental Materials:**

2 **Supplemental Methods:**

3 **Wound healing assay.** Cells were pre-treated with epinephrine for 5 days and then plated in
4 six-well plates and grew to confluent cell monolayers. Subsequently, three horizontal scratches
5 were made gently with sterile pipette tip across the diameter of the well and then incubated in
6 serum-free medium. For each well, at least five pictures were taken microscopically at 0 h and 48
7 h after scratching. The percentage of wound healing was determined based on three
8 measurements of the wound area.

9 **Transwell invasion assay.** Cells were pre-treated with epinephrine for 5 days. Then cells ($2 \times$
10 10^4) resuspended in serum-free medium were placed in 50 μ l matrigel (BD Biosciences) coated
11 membrane in upper chamber (24-well insert, 8 μ m, Corning Costar, China) and incubated for 36
12 h. Medium supplemented with 10% FBS were used as an attractant in the lower chamber. After
13 being incubated for 36 h, cells invaded through the membrane were fixed with 4%
14 paraformaldehyde (Santa Cruz) and stained with 0.5% crystal violet (Shanghai Sangon Company,
15 China). The stained cell images were captured by microscope (Olympus, Japan), and five
16 random fields at 10 \times magnification were counted.

17 **Transwell migration assay.** Cells were pre-treated with epinephrine for 5 days. Then cells (5
18 $\times 10^4$) resuspended in serum-free medium were placed into uncoated membrane in the upper
19 chamber (24-well insert, 8 μ m, Corning Costar, China). Growth medium supplemented with 10%
20 FBS was used as an attractant in the lower chamber. After being incubated for 24 h, cells
21 migrated through the membrane were fixed with 4% paraformaldehyde (Santa Cruz, USA) and
22 stained with 0.5% crystal violet (Shanghai Sangon Company, China). The stained cell images

1 were captured by microscope (Olympus, Japan), and five random fields at 10× magnification
2 were counted.

3 ***Chromatin immunoprecipitation (ChIP).*** Cells (1×10^7) were fixed with 1% formaldehyde
4 for 10 min at room temperature. Next, 10× glycine was added to the fixation solution to inhibit
5 crosslinking. Cells were collected in PBS at 4°C, centrifuged at 1,000 ×g for 5 min, resuspended
6 in 1 ml ice-cold 1% SDS buffer and lysed on ice for 30 min. The cells were homogenized on ice
7 to aid release of nuclei. Cells were sonicated for 10 min at 7 watts average incident power
8 (Covaris). Chromatin (25 μg) was immunoprecipitated for 12 h with 2 mg of specific antibodies
9 directed against MYC (Abcam) and Protein G magnetic beads (25 ml). Beads were then washed
10 sequentially for 5 min with the following buffers: once with ChIP Buffer I and twice with ChIP
11 Buffer II. Immune complexes were eluted in 50 ml elution buffer AM2. Supernatants were
12 reverse cross-linked by heating at 65°C for 12 h, treated with 1 ml RNaseA at 37°C for 15 min
13 and digested with 2 ml proteinase K at 37°C for 1 h. DNA was obtained by phenol and
14 phenol/chloroform extraction. The human *SLUG* promoter-specific primers used for PCR are
15 listed in Supplemental Table F.

16 ***Extracellular Acidification Rate and Oxygen Consumption Rate Assays.*** The extracellular
17 acidification rate (ECAR) and cellular oxygen consumption rate (OCR) were measured using the
18 Seahorse XFe 24 Extracellular Flux Analyzer (Seahorse Bioscience). Experiments were
19 performed according to the manufacturer's instructions. Briefly, cells were treated with
20 epinephrine for 5 days and cell number was determined. Fifty thousand cells per well were then
21 seeded into a Seahorse XF 24 cell culture microplate for 10 h, at which time cell number for each
22 group was very similar. Cells were used for measurement of ECAR and OCR. Baseline
23 measurements were collected. Then, for ECAR analysis, glucose, the oxidative phosphorylation

1 inhibitor oligomycin and the glycolytic inhibitor 2-DG were sequentially injected into each well
2 at the indicated time points. For OCR, oligomycin, the reversible inhibitor of oxidative
3 phosphorylation FCCP (p-trifluoromethoxy carbonyl cyanide phenylhydrazone) and the
4 mitochondrial complex I inhibitor rotenone plus the mitochondrial complex III inhibitor
5 antimycin A (Rote/AA) were sequentially injected. Data were analyzed using Seahorse XF-24
6 Wave software. OCR was reported in pmols/minute and ECAR in mpH/minute. The results were
7 normalized to cell number.

8 ***Behavioral analyses.*** To assess the effects of chronic stress on locomotor and exploratory
9 activities, mice were evaluated in an open field test. The open field was constructed of plywood
10 and surrounded by walls 30 cm in height. The floor of the open field was 50 cm in length and
11 50 cm in width. Each mouse was placed individually at the center of the apparatus and was
12 observed for 6 min to record locomotor activity (1). Total duration of immobility and latency
13 induced by tail suspension were measured (2). Mice were suspended 45 cm above the floor by an
14 adhesive tape placed approximately 1 cm from the tip of the tail. Time of immobility and latency
15 was recorded during a 6-min period (3). All results were recorded and analyzed using Xeye Aba
16 V3.2 software.

17 ***Molecular Dynamics Simulation.*** 1) USP28 and MYC modeling. The homology modeling
18 program MODELLER 9.17 was used for characterizing USP28 and MYC motifs (AA: 46-74;
19 confirmed by prior pull-down experiments (4, 5)) followed by MD optimization; 2) Protein
20 Docking and MD simulation. We used the Zdock program to perform global rigid-body docking
21 for USP28^{WT} or USP28^{C171A} complexed with the MYC⁴⁶⁻⁷⁴ motif. All the MD simulations were
22 performed using Gromacs 4.6.7 with the Amber99sb force field; 3) Free energy surface (FES)

1 analysis. Free energy surfaces were obtained by integrating the deposited bias during
2 metadynamics protocol implemented in the PLUMED program.

3 ***Prediction of Transcription Factor Binding Sites.*** Transcription factor binding sites were
4 predicted using JASPAR 2014 software (<http://jaspar.genereg.net/>) (6). Since sensitivity and
5 specificity are affected by the relative score threshold (default 80%), the submitted sequences
6 were analyzed using a relative profile score threshold setting of 90% to the “CORE Vertebrata”
7 database. This approach reports only the most likely sites (7) because experimentally reported
8 binding sites in DNA frequently locate true sites as the highest-scoring sequences (8). Position
9 frequency matrix cell numbers indicate the number of sequences with base x in column y.
10 Sequence logos (9) are graphical representations of a transcription factor consensus binding site,
11 in which nucleotides are sized and sorted relative to their occurrence at each position. The ranges
12 are from 0 (no base preference) to 2 (single base occurrence).

13 ***Constant-pH molecular dynamics simulations (CpHMD).*** To delineate the effects of
14 increased lactate product (the change of solvent pH), we employed constant-pH MD simulations
15 (CpHMD) (10) to model the interactions of USP28 with MYC motif mimicking titration
16 experiments at atomic level. The newest version of Amber16 and AmberTool17 (11) were used
17 for CpHMD study with the AMBER99 force field and the GB implicit solvent model. In the
18 present study, we used the distance of MYC^{Lys51} to USP28^{C171-H600} to measure the binding
19 capabilities of potential ubiquitin ligated sites in MYC motif with the catalytic domain of USP28.
20 The pH 6.4 condition clearly enables a more stable interaction between MYC motif with the
21 USP28 than that in neutral pH 7.4. Interestingly, in acidic pH 4.0 or basic pH 9.0 condition, the
22 binding between MYC motif with USP28 appears unstable and fluctuates with increased
23 frequency of dissociations.

1 ***Virtual screening of FDA-approved drugs against LDHA.*** Our in-house docking program
2 FIPSDock63 was used to perform the virtual screening of 2037 FDA-approved small molecule
3 drugs against LDHA. Noteworthy, vitamin C stands out in the vitamins group (seven hits) among
4 top 200 hits in the virtual screening campaign.

5 ***MTT assay.*** MDA-MB-231 cells (2×10^3) were plated onto 96-well flat bottom plates in a
6 final volume of 100 μ l/well. After attached, cells were exposed to test compounds for times
7 indicated and viability examined at 490 nm.

8 ***Microarray analysis.*** Total RNA was extracted by Trizol and submitted to the Gene Tech
9 Company Limited (Shanghai, China) for labelling and hybridization for 16 h at 45°C using
10 Affymetrix Clariom D. Microarray scans were obtained with a GeneChip Scanner 3000 7G
11 (Affymetrix, Santa Clara, CA) using the default settings. Data were normalized with the Robust
12 Multichip Analysis (RMA) algorithm using default analysis settings and some additional
13 median/quantile normalization. We then eliminated all probes with a mean < 6.0 and standard
14 deviation < 1.0 to filter the number of probes from 49,293 to 26,000. Then, we normalized the
15 data with a fold change > 2 and P value < 0.05 (117 genes). We further selected the data with a
16 fold change > 2 and Q value < 0.05 by the method with Benjamini-hochberg, resulting in 54
17 genes being chosen, and which were included in the 117 genes. Gene Ontology Enrichment
18 analysis was performed in the website (<https://david.ncifcrf.gov>).

19 ***Gene set enrichment analysis (GSEA).*** We searched the publicly available databases to
20 identify differential gene expression between cancer stem cells (CSCs) and non-CSCs with
21 replicates. Four GEO datasets GSE65576 (bulk tumor cells and spheroid-cultured cell with stem
22 cell medium from glioblastoma samples), GSE33874 (side population (SP) and main population
23 (MP) of human ovarian adenocarcinoma samples), GSE36563 (SP and MP samples of

1 xenografts which derived from human pancreatic ductal adenocarcinoma samples) and
2 GSE59281 (CD44⁺/CD24^{low} and CD44⁺/CD24⁻ breast cancer cell line) were subsequently
3 selected and analyzed by GEO2R.

4

1 **References**

- 2 1. Rodrigues AL, et al. Involvement of monoaminergic system in the antidepressant-like effect
3 of the hydroalcoholic extract of *Siphocampylus verticillatus*. *Life Sci.* 2002;70(12):1347-
4 1358.
- 5 2. Steru L, Chermat R, Thierry B, Simon P. The tail suspension test: a new method for screening
6 antidepressants in mice. *Psychopharmacology (Berl)*. 1985;85(3):367-370.
- 7 3. Tomida S, et al. *Usp46* is a quantitative trait gene regulating mouse immobile behavior in the
8 tail suspension and forced swimming tests. *Nat Genet.* 2009;41(6):688-695.
- 9 4. Popov N, et al. The ubiquitin-specific protease *USP28* is required for *MYC* stability. *Nat Cell*
10 *Biol.* 2007;9(7):765-774.
- 11 5. Diefenbacher ME, et al. *Usp28* counteracts *Fbw7* in intestinal homeostasis and cancer.
12 *Cancer Res.* 2015;75(7):1181-1186.
- 13 6. Mathelier A, et al. JASPAR 2014: an extensively expanded and updated open-access
14 database of transcription factor binding profiles. *Nucleic Acids Res.* 2014;42(Database
15 issue):D142-147.
- 16 7. van den Hoven R, Gur E, Schlamanig M, Hofer M, Onmaz AC, Steinborn R. Putative
17 regulation mechanism for the *MSTN* gene by a CpG island generated by the SINE marker
18 *Ins227bp*. *BMC Vet Res.* 2015;11:138.
- 19 8. Benitez-Bellon E, Moreno-Hagelsieb G, Collado-Vides J. Evaluation of thresholds for the
20 detection of binding sites for regulatory proteins in *Escherichia coli* K12 DNA. *Genome Biol.*
21 2002;3(3):RESEARCH0013.
- 22 9. Schneider TD, Stephens RM. Sequence logos: a new way to display consensus sequences.
23 *Nucleic Acids Res.* 1990;18(20):6097-6100.

- 1 10. Mongan J, Case DA, McCammon JA. Constant pH molecular dynamics in generalized Born
2 implicit solvent. *J Comput Chem.* 2004;25(16):2038-2048.
- 3 11. Case DA, et al. The Amber biomolecular simulation programs. *J Comput Chem.*
4 2005;26(16):1668-1688.
- 5

1 **Supplemental Table 1:**

Antibodies		
REAGENT or RESOURCE	SOURCE	Catalog
β-Catenin (Rabbit monoclonal)	Cell Signaling Technology	Cat#8480
NANOG (Rabbit polyclonal)	Abcam	Cat#ab80892
OCT-4 (Mouse monoclonal)	Cell Signaling Technology	Cat#75463
ADRB1 (Rabbit polyclonal)	Abcam	Cat#ab3442
ADRB2 (Rabbit monoclonal)	Abcam	Cat#ab182136
SLUG (Rabbit polyclonal)	Abcam	Cat#27568
MYC (Rabbit or Mouse monoclonal)	Cell Signaling Technology or Abcam (ChIP)	Cat#5605S or Cat#ab32
USP28 (Rabbit polyclonal)	Proteintech	Cat#17707-1-AP
LDHA (Rabbit monoclonal)	Cell Signaling Technology	Cat#3582S
PKM2 (Rabbit monoclonal)	Cell Signaling Technology	Cat#4053S
PDK1 (PDHK1) (Rabbit monoclonal)	Cell Signaling Technology	Cat#3820S
PFKM (Rabbit polyclonal)	Proteintech	Cat#55028-1-AP
HK2 (Rabbit monoclonal)	Cell Signaling Technology	Cat#2106S
HA (Rabbit monoclonal)	Proteintech	Cat#51064-2-AP
TWIST1 (Rabbit polyclonal)	Proteintech	Cat#25465-1-AP
SNAIL(Rabbit polyclonal)	Abcam	Cat# ab180714
Ubiquitin (Mouse monoclonal)	Cell Signaling Technology	Cat#3936
GAPDH (Mouse monoclonal)	Proteintech	Cat#60004-1-Ig
Goat anti-Mouse IgG Secondary Antibody	Thermo Fisher Scientific	Cat#31430
Goat anti-Rabbit IgG Secondary Antibody	Thermo Fisher Scientific	Cat#31460

2

1 **Supplemental Table 2:**

Chemicals, Peptides and Recombinant Proteins		
REAGENT or RESOURCE	SOURCE	Catalog
MG132	Selleck	Cat#S2619;
Protein A/G PLUS-Agarose Immunoprecipitation Reagent	Santa Cruz	Cat#sc2003
Cycloheximide	Coolaber	Cat#CC4071;
Lipofectamine 2000	Invitrogen	Cat#11668-019
Puromycin Dihydrochloride	ThermoFisher	Cat#A1113803;
Atenolol	Sigma	Cat#A7655-1G;
ICI118,551 hydrochloride	Sigma	Cat#I127;
TRIzol reagent	Life Technologies	Cat#15596-026
Epinephrine bitartrate	Selleck	Cat#S2521
Propranolol hydrochloride	Sigma	Cat#P0884;
Norepinephrine	Isoreag	Cat#IR-15054S
Cortisol	Sigma	Cat#C-113
Actinomycin D	Abmole	Cat#M4881;
SYBR Select Master Mix	Life Technologies	Cat#4472908
EasyScript One-Step gDNA Removal cDNA Synthesis SuperMix	Transgen	Cat#AE311-03
B27	Life Technologies	Cat#17504-044
bFGF	PEPROTECH	Cat#100-18B
EGF (hEGF)	Sigma	Cat#E9644;
Sodium Oxamate	Sigma	Cat#O2751;
L-(+)-Lactic acid	Sigma	Cat#L1750;
L-Ascorbic acid	Sigma	Cat#V900134;

2

1 **Supplemental Table 3:**

Critical Commercial Assays		
REAGENT or RESOURCE	SOURCE	Catalog
WesternBright TM MECL kit	Advansta	K-12045-D50
DAB kit	ZSGB-BIO	ZLI-9018
Dual-Luciferase [®] Reporter Assay System	Promega	E1910
ChIP-IT Express Chromatin Immunoprecipitation Kits	Active Motif	53008
SPlink Detection Kits	ZSGB-BIO	SP-9000
Glucose uptake	BioVision	K606-100
Lactate production	BioVision	K627-100
ATP levels were measured by assay kits	BioVision	K354-100
Cell Mito Stress Test Kit	Agilent	103015-100
Glycolysis Stress Test Kit	Agilent	103020-100

2

1 **Supplemental Table 4:**

Experimental Models: Cell Lines		
REAGENT or RESOURCE	SOURCE	Catalog
MDA-MB-231	ATCC	Cat# CRM-HTB-26
MCF-7	ATCC	Cat# HTB-22™
293T	ATCC	Cat#CRL-3216™
Py8119	Fudan University Shanghai	
E0771	BeNa Culture Collection	BNCC342034

2

1 **Supplemental Table 5:**

Experimental Models: Organisms/Strains		
NOD/SCID mouse model	Female	Beijing Vital River Laboratory Animal Technology Co., Ltd.
BALB/C mouse model	Female	Beijing Vital River Laboratory Animal Technology Co., Ltd.
C57BL/6 mouse model	Female	Dalian Medical University

2

1 **Supplemental Table 6:**

Oligonucleotides		
RT-q-PCR (Sangon Biotech)	sense (5'-3')	antisense (5'-3')
MYC	TCAAGAGGCGAACACACAAC	GGCCTTTTCATTGTTTTCCA
SLUG	ATGAGGAATCTGGCTGCTGT	CAGGAGAAAATGCCTTTGGA
POU5F1	GAGAACCGAGTGAGAGGCAACC	CATAGTCGCTGCTGATCGCTTG
CTNNB1	ATGGAGCCGGACAGAAAAGC	TGGGAGGTGTCAACATCTTCTT
NANOG	CCAAATTCTCTGCCAGTGAC	CACACGTCTTCAGGTTGCAT
ABCG2	ATCAGCTGGTATCACTGTGAGGCC	AGTGGCTTATCCTGCTTGAAGGC
TFAP2C	GAAGAGGACTGCGAGGATCG	GCTGATATTCGGCGACTCCA
BMP4	GGAGGAGGAGGAAGAGCAGA	CACTGGTCCCTGGGATGTTT
WISP2	CTGGCCTTGTCTCTTCCCTG	AGAAGCGGTTCTGGTTGGAC
NDRG1	AGGAGCAGGACATCGAGACT	CGATGTCATGGTAGGTGAGG
HS3ST1	ATGCACACATGCTGAACTGG	GCAGTAGAAGCCCTTGGTTTTG
TMCC3	AAGAGCCGGGTAGAACGTCAT	TCAAAGTTGAGGTTGGTGTCTG
LDHA	CACCAAAGATTGTCTCTGGCA	AAGATGTTACGTTACGCTGG
USP28	GGACCCTTCCTTTCTCCATGA	AGGCTGACTGCCTGAGTAATGTC
ACTB	TTGCCGACAGGATGCAGAAGGA	AGGTGGACAGCGAGGCCAGGAT
PCR (ChIP) (Sangon Biotech)	sense (5'-3')	
SNAI2-pro0-R	CTTGCCAGCGGGTCTGGCGG	
SNAI2-pro394-F	CTCACCGAGCGAGGTTACCT	
SNAI2-pro394-R	CCCCGCCCGGATCCACGCTC	
SNAI2-pro496-F	GCGCGCTGGCGCTGCACCACA	

2

1 Supplemental Table 7:

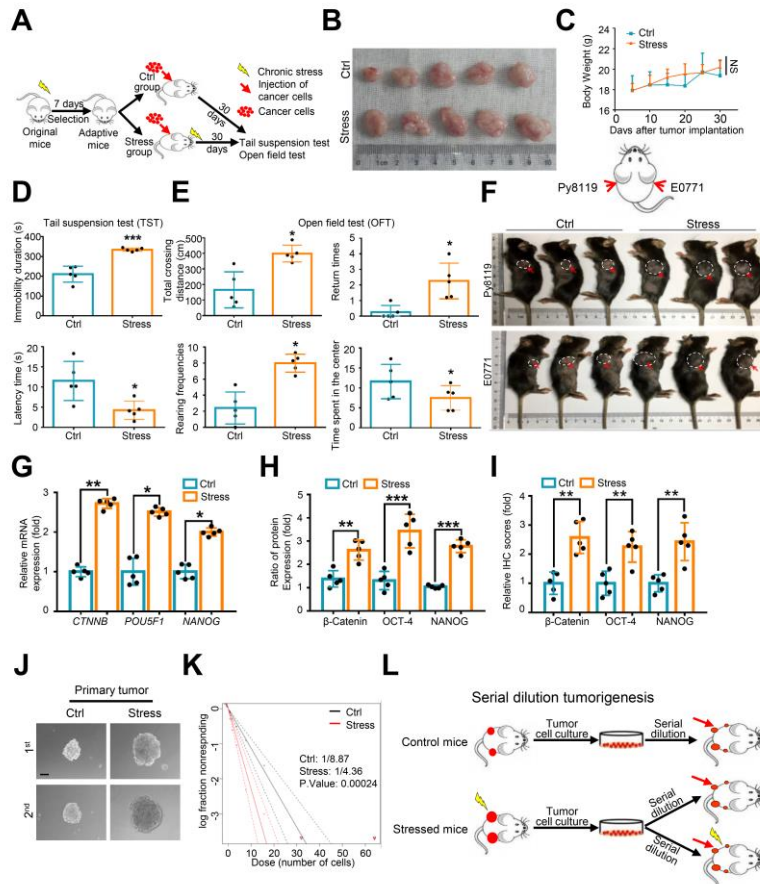
Oligonucleotides		
siRNAs (GenePharma, Suzhou, China)	sense (5'-3')	
siNC	5'-UUCUCCGAACGUGUCACGU-3'	
siUSP28-1	5'-ACUCAGACUUAUGAACAGAUACUGC-3'	
siUSP28-2	5'-CUGCAUGCAAGCGAUAAGG-3'	
siUSP28-3	5'-CUGCAUUCACCUUAUCAUU-3'	
siADRB2-1	5'-GCCAUUACUUCACCUUUCA-3'	
siADRB2-2	5'-GCCUAGCGAUAAACAUUGAU-3'	
siADRB2-3	5'-CGCCCAUUAUCUUAUGAAA-3'	
siADRB2-4	5'-CAGAGUGGAUAUCACGUGGAA-3'	
siADRB1-1	5'-CCGCUGUCUCAGCAGUGGA-3'	
siADRB1-2	5'-CGCUCACCAACCUCUUCAU-3'	
siADRB1-3	5'-CCUCGUCCGUAGUCUCCUU-3'	
siADRB1-4	5'-CCGAUAGCAGGUGAACUCGAA-3'	
siLDHA	5'-GGCAAAGACUAAAUGUAA-3'	
siHK2	5'-CCTGGGTGAGATTGTCCGTAA-3'	
shRNA	sense (5'-3')	antisense (5'-3')
shSLUG-1	CCGGCCATTCTGATGTAAAGAAATCT CGAGATTCTTTACATCAGAATGGGTTT TT	AATTA AAAACCCATTCTGATGTAAAGA AATCTCGAGATTCTTTACATCAGAATG GG
shSLUG-2	CCGGCCGAAGCCAAATGACAAATAACT CGAGTTA TTTGTCATTTGGCTTCGGTTT TT	AATTA AAAACCGAAGCCAAATGACAAA TAACTCGAGTTA TTTGTCATTTGGCTTC GG
shSLUG-3	CCGGGAGTGACGCAATCAATGTTTACT CGAGTAAACATTGATTGCGTCACTCTTT TT	AATTA AAAAGAGTGACGCAATCAATGT TTACTCGAGTAAACATTGATTGCGTCAC TC
shMYC-1	CCGGCCAAGGTAGTTATCCTTAAACT CGAGTTTAAGGATAACTACCTTGGGTTT TT	AATTA AAAACCCAAGGTAGTTATCCTTA AACTCGAGTTTAAGGATAACTACCTTG GG
shMYC-2	CCGGACTGAAAGATTTAGCCATAATCT CGAGATTATGGCTAAATCTTTCAGTTTT TT	AATTA AAAAACTGAAAGATTTAGCCAT AATCTCGAGATTATGGCTAAATCTTTC AGT

2

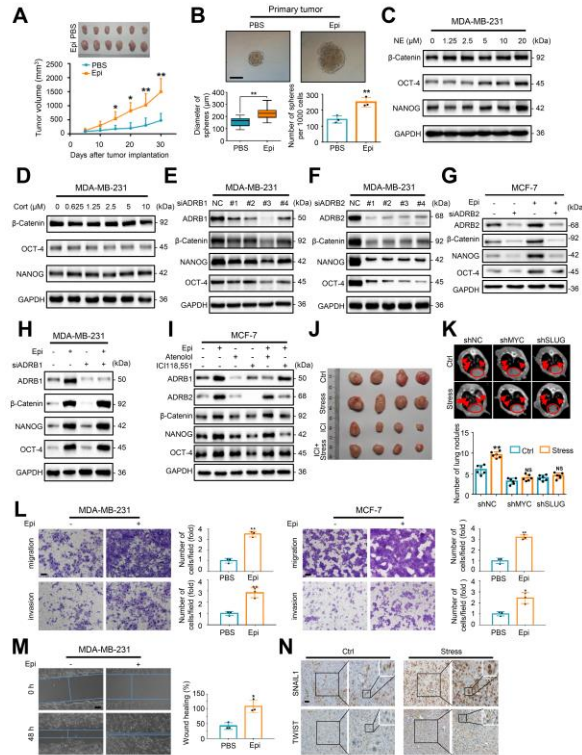
1 **Supplemental Table 8:**

Oligonucleotides		
Plasmid	forward primer (5'-3')	reverse primer (5'-3')
plvx-SNAI2	CCGGAATTCGCCACCATGCCGCGCTCCTTCCTGGT	CGGGATCCTCAGTGTGCTACACAGCAGC
plvx-SNAI2-Red	CCGGAATTCGCCACCATGCCGCGCTCCTTCCTGGT	CGGGATCCCGGTGTGCTACACAGCAGCCAG
PCS2-SLUG	CAGGATCCGCCACCATGCCGCGCTCCTTCCTGGT	TTGAATTCCTCAGTGTGCTACACAGCAGCCAG
pcDNA6-His-SLUG	CAGGATCCGCCACCATGCCGCGCTCCTTCCTGGT	CAGAATCCCGGTGTGCTACACAGCAGCCAG
Luciferase constructs	forward sense (5'-3')	reverse sense (5'-3')
pGL3-basic-SNAI2 1k	CGGGGTACCAAAGATAAGATCTCTGTGTC	CCGCTCGAGCTTGCCAGCGGGTCTGGCG
pGL3-basic-SNAI2 1.5k	CGGGGTACCGACAATGCACTTTTCTCTG	CCGCTCGAGCTTGCCAGCGGGTCTGGCG
pGL3-basic-SNAI2 2k	CGGGGTACCTGGATTATGCTCTGTGATCC	CCGCTCGAGCTTGCCAGCGGGTCTGGCG
pGL3-basic-SNAI2 Mut1	TAGGGACCGCAAAATCCTCCCGCC	GGCGGGAGGAAAAAGCGGTCCCTA
pGL3-basic-SNAI2 Mut2	CGCACCTGAGAAAAGCCCCTGCC	GGCAGGGGCAAAAAGCTCAGGTGCG
pGL3-basic-SNAI2 Mut3	TCCCAGAGAGAAAAATCGCGGGCG	CGCCCGGATAAAAAGCTCTCTGGGA
pGL3-basic-POU5F1 2k	CGGGGTACCCCTGGCCAGAGCCCTC	CATGCCATGGGAAGGAAGGCGCCCAAGC

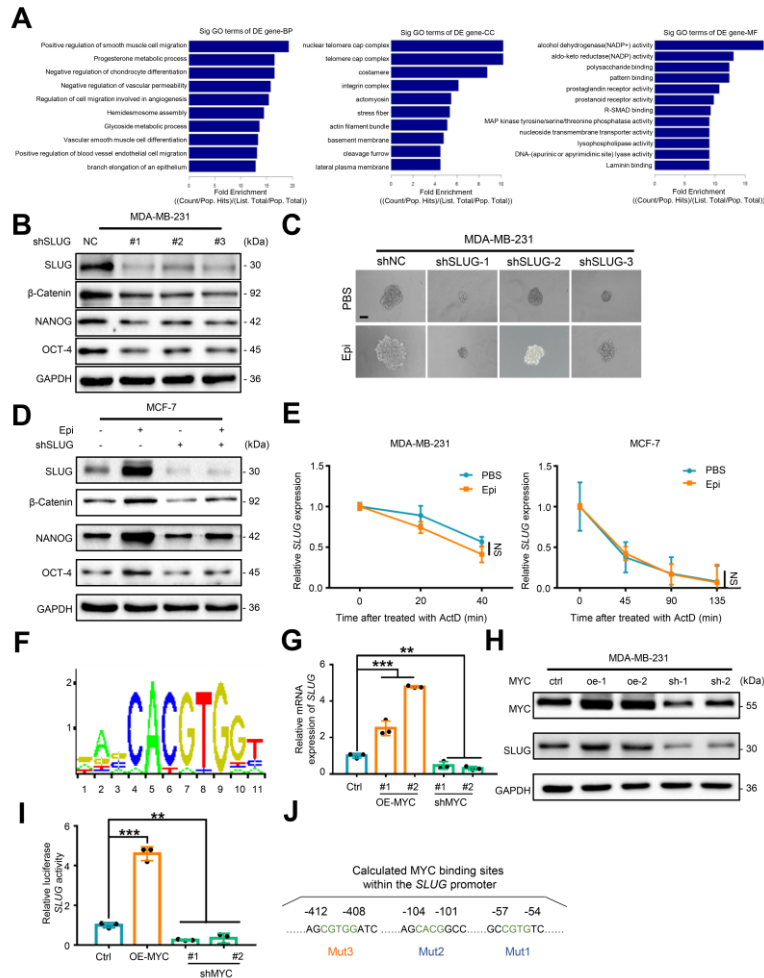
2



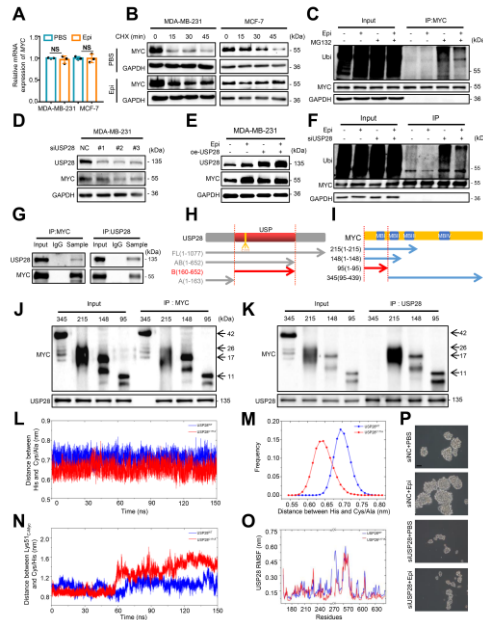
2
3 **Supplemental Figure 1. Chronic stress promotes CSC-like properties in mouse model.** (A)
4 Schematic diagram of the chronic stress mouse model. The yellow flash indicates chronic stress,
5 the red arrow indicates injection of cancer cells and the red dots indicate cancer cells. (B)
6 Representative tumor image of MDA-MB-231 tumors in Control (Ctrl) and Stressed mice; n=5.
7 (C) Body weight growth curves of mice over 30 days following tumor implantation. n=5 (1-way
8 ANOVA). (D) Mice were subjected to behavioral tests after completion of the chronic stress
9 paradigm. Immobility duration (upper panel) and latency time (lower panel) were analyzed by
10 the tail suspension test. n=5 (1-way ANOVA). (E) Total crossing distance (upper-left panel),
11 return times (upper-right panel), rearing frequencies (lower-left panel) and time spent in the
12 center (lower-right panel) were analyzed with an open field test. n=5 (1-way ANOVA). (F)
13 Diagram of Py8119 and E0771 cells injected sites (upper panel) and representative tumor images
14 from control (Ctrl) and stressed (Stress) mice injected with these tumor cell lines (bottom panel),
15 n= 6. (G and H) Relative mRNA levels (G) and protein levels (H) of selected proteins in tumor
16 cells from Ctrl- or stress-induced mice. Intensity of protein expression was quantified by
17 densitometry and differences expressed as fold changes. n=5 (Student's *t* test). (I) IHC scores of
18 indicated proteins from Ctrl- and stress-induced tumor tissue. n=5 (Student's *t* test). (J)
19 Representative images of primary and secondary sphere formation of primary MDA-MB-231
20 tumors from the Ctrl and Stress groups. Scale bar, 50 μm (K) Limiting dilution assay of Ctrl and
21 stressed MDA-MB-231 xenografted tumor cells. n=3 (χ² test). (L) Serially diluted tumor cells
22 were subcutaneously inoculated at 4 different sites into each mouse. Data are representative of 3
23 independent experiments. Data represent mean ± SEM, *p < 0.05, **p < 0.01, ***p < 0.001.



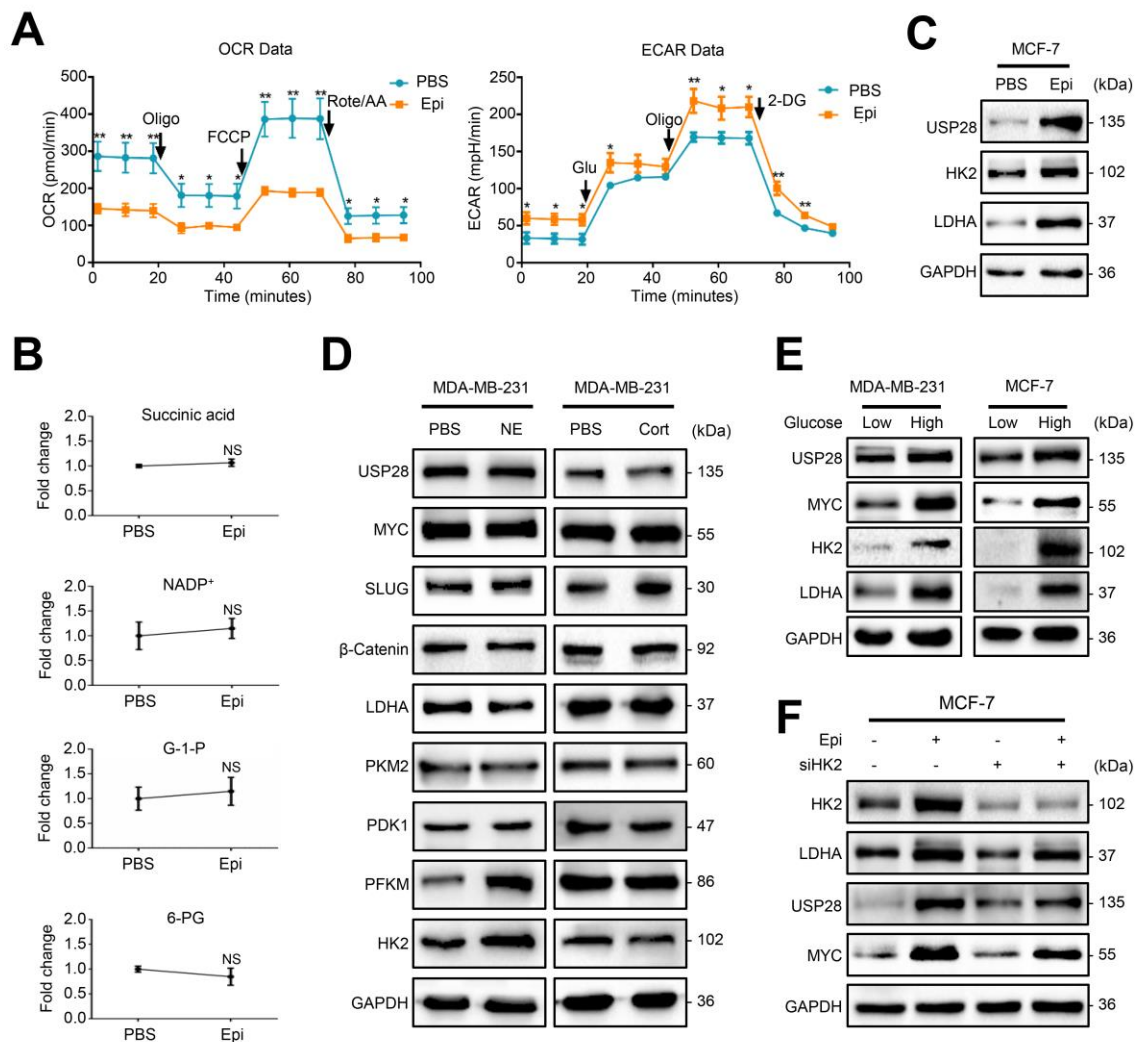
1
 2 **Supplemental Figure 2. Epinephrine promotes CSC-like traits via ADRB2.** (A)
 3 Representative tumor image derived from PBS- and Epi-treated mice (upper panel). Scale bar, 1
 4 cm (1-way ANOVA). Tumor growth curves are shown (lower panel). n=6. (B) Representative
 5 spheroid images derived from PBS- and epinephrine (Epi)-induced tumors cells (upper panel).
 6 Scale bar, 100 μ m. Bottom left panel shows distribution pattern of mammosphere size from
 7 tumor cells. Bottom right panel shows the number of mammospheres (d > 50 μ m); n=3 (1-way
 8 ANOVA). (C and D) Immunoblot analysis with indicated antibodies in MDA-MB-231 cells
 9 treated with increasing concentrations of NE (C) and Cort (D). (E and F) MDA-MB-231 cells
 10 were transfected with 4 different siRNAs targeting ADRB1 (E) or targeting ADRB2 (F). Cell
 11 lysates were analyzed for the expression of indicated proteins. (G) MCF-7 cells were transfected
 12 with siADRB2 and then treated with Epi for 5 days. Expression of proteins was determined by
 13 immunoblot analysis. (H) MDA-MB-231 cells were transfected with siRNA targeting ADRB1
 14 with or without Epi for 5 days. Cell lysates were analyzed for the expression of indicated
 15 proteins. (I) MCF-7 cells were treated with PBS, atenolol (A), or ICI18,551 (ICI) in the
 16 presence or absence of Epi for 5 days. Immunoblot analysis was used to analyze the expression
 17 of indicated proteins in the cell lysates. (J) Representative tumor image derived from Ctrl or
 18 stressed mice in the presence or absence of ICI. n=5. (K) Representative images of CT scan of
 19 mice with indicated treatments. Statistical significance was determined by one-way ANOVA test
 20 (n=6). (L) Representative images of MDA-MB-231 and MCF-7 cells in transwell assays.
 21 Statistical significance was determined by one-way ANOVA test. n=3, Scale bar, 100 μ m. (M)
 22 Representative images of MDA-MB-231 cells in wound healing assay. Statistical significance
 23 was determined by one-way ANOVA test. n=3. Scale bar, 100 μ m. (N) Representative IHC
 24 staining for indicated antibodies of Ctrl and stressed tumor tissue. n=5, Scale bar, 50 μ m. Data
 25 are representative of at least 3 independent experiments. Data represent mean \pm SEM, *p < 0.05,
 26 **p < 0.01.



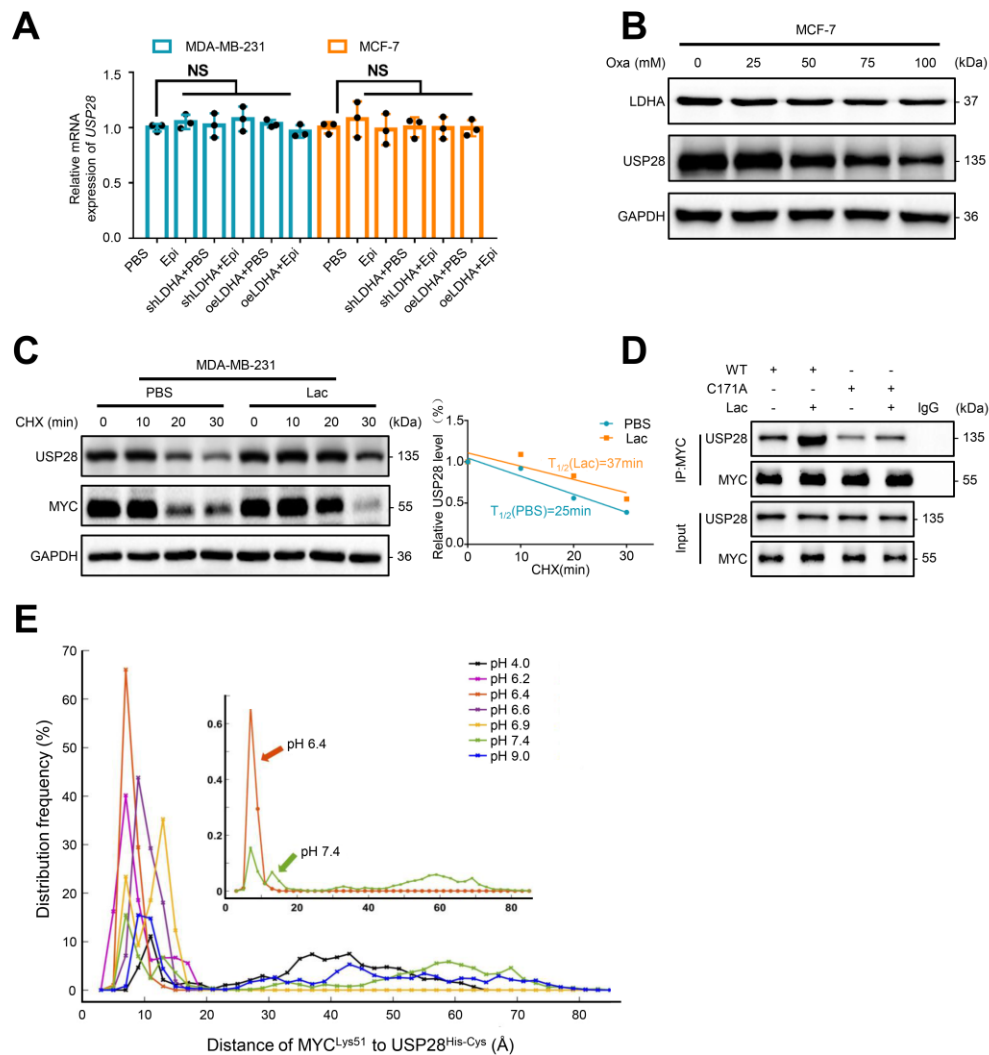
1
2 **Supplemental Figure 3. Epinephrine transactivates SLUG via MYC.** (A) Gene set
3 enrichment analysis of 117 altered genes (fold change > 2 and P value < 0.05) showing the top
4 10 most-enriched gene sets. (B) Immunoblot analysis of MDA-MB-231 cells transfected with 3
5 different shRNAs targeting SLUG. (C) Representative images of mammospheres from shNC or
6 shSLUGs MDA-MB-231 cells and treated with PBS or Epi for 5 days. n=3. Scale bar, 50 μm. (D)
7 MCF-7 cells were transfected with shRNA-1 targeting SLUG in the presence or absence of Epi
8 for 5 days. Cell lysates were subjected to immunoblot analysis for selected proteins. (E) MDA-
9 MB-231 and MCF-7 cells were treated with Epi for 5 days. Actinomycin D (ActD) was added
10 for the indicated times before cells were harvested. Half-life of mRNAs for each treatment was
11 predicted as described. n=3 (1-way ANOVA). (F) Prediction of transcription factor binding site
12 in the SLUG promoter using the JASPAR database. (G and H) MDA-MB-231 cells were
13 transfected with MYC overexpression (oe-1, oe-2) or knockdown (sh-1, sh-2) vectors, mRNA
14 levels were verified by RT-qPCR (G). n=3 (1-way ANOVA). Cell lysates were subjected to
15 immunoblot analysis with the indicated antibodies (H). (I) MDA-MB-231 cells were transfected
16 with ctrl or oe-MYC or MYC shRNA for 48 h, and then transfected with a pGL3-SLUG (-496~0)
17 truncated promoter. After 24 h, cells were harvested for dual-luciferase analysis. n=3 (1-way
18 ANOVA). (J) Schematic diagram of SLUG WT, mutant 1 (Mut1, -57 to -54), mutant 2 (Mut2, -
19 104 to -101), or mutant 3 (Mut3, -412 to -408). Data are representative of at least 3 independent
20 experiments. Data represent mean ± SEM, **p < 0.01, ***p < 0.001.



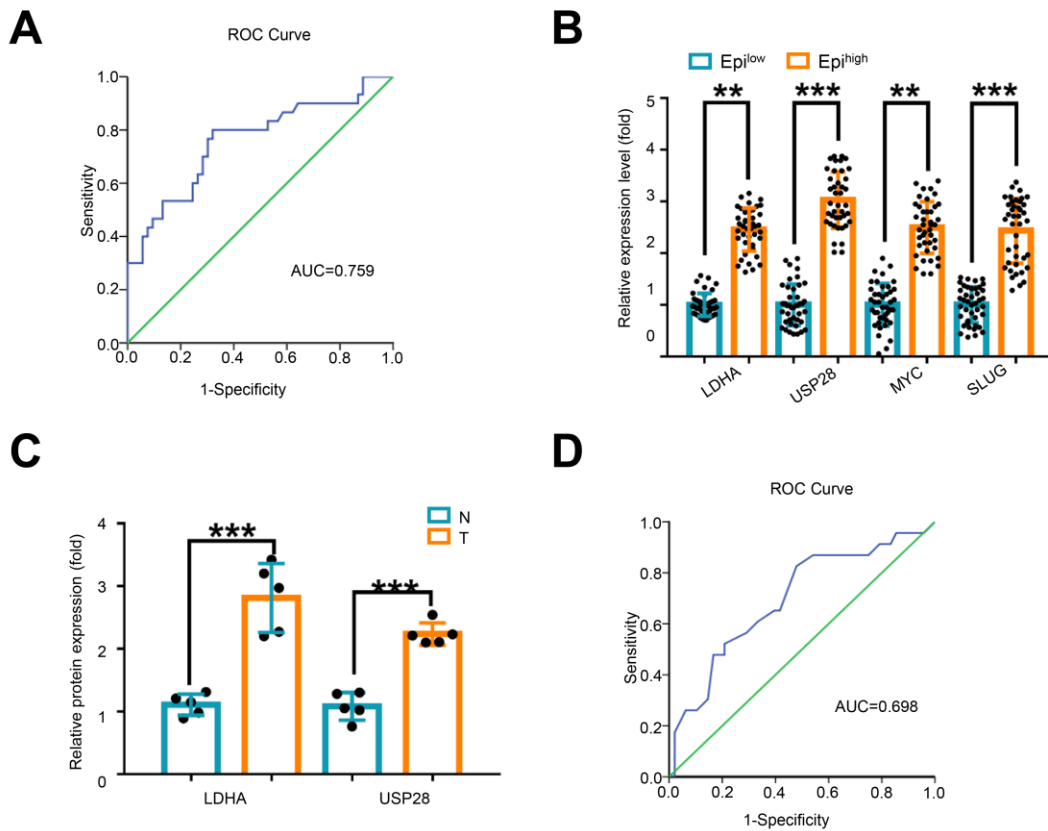
1
2 **Supplemental Figure 4. Epinephrine stabilizes MYC via USP28 deubiquitination.** (A)
3 MDA-MB-231 and MCF-7 cells were treated with PBS or Epi for 5 days. Expression of MYC
4 mRNA was verified by RT-qPCR. n=3 (Student's *t* test). (B) Immunoblots of cancer cells treated
5 with Epi for 5 days followed by treated with cycloheximide (CHX) for the indicated times. (C)
6 Ubiquitin assays of 293T cells transfected with ubiquitin (UB) and MYC followed by treated
7 with Epi and/or MG132. (D) Immunoblot analysis of MDA-MB-231 cells transfected with 3
8 different shRNAs targeting USP28. (E) MDA-MB-231 cells were transfected with oe-USP28
9 and then treated with PBS or Epi for 5 days. Expression of the indicated proteins was examined
10 by immunoblotting. (F) MYC and HA-UB were co-expressed with siRNA-2 targeting USP28 in
11 the presence or absence of Epi in 293T cells. MYC was immunoprecipitated and the
12 polyubiquitination of MYC was detected by immunoblotting. (G) MYC and USP28 were
13 transfected into 293T cells. MYC and USP28 were immunoprecipitated with a MYC or USP28
14 antibody, respectively, and USP28 and MYC were analyzed by immunoblotting. (H) Schematic
15 diagram of USP28 structure and deletion constructs. (I) Schematic diagram showing the structure
16 of MYC and deletion constructs that were used. (J and K) Deletion mutants of MYC were co-
17 expressed with USP28 in 293T cells. Extracts were immunoprecipitated with MYC (J) or USP28
18 (K) antibody Bound USP28 or MYC was then examined by immunoblotting. (L) Distance
19 between His⁶⁰⁰ and the Cys/Ala mutation site in USP28 during a 150-ns MD simulation. The
20 USP28^{WT} profile is displayed in blue and the USP28^{C171A} profile is depicted in red. (M)
21 Frequency distribution histogram for the distance between His⁶⁰⁰ and Cys/Ala mutation site in
22 USP28 during a 150-ns MD simulation. The USP28^{WT} profile is displayed in blue and the
23 USP28^{C171A} profile is shown in red. (N) Distance between the center of mass of MYC^{Lys51} and
24 center of mass of USP28^{His-Cys/Ala} during a 150-ns MD simulation. The USP28^{WT} profile is
25 shown in blue and the USP28^{C171A} profile is shown in red. (O) RMSF profiles for USP28^{WT} and
26 USP28^{C171A} during a 150-ns MD simulation. (P) Representative spheroid images formed by cells
27 transfected with USP28 siRNA-2 followed by treated with PBS or Epi for 5 days. Data are
28 representative of at least 3 independent experiments. Data represent mean ± SEM.



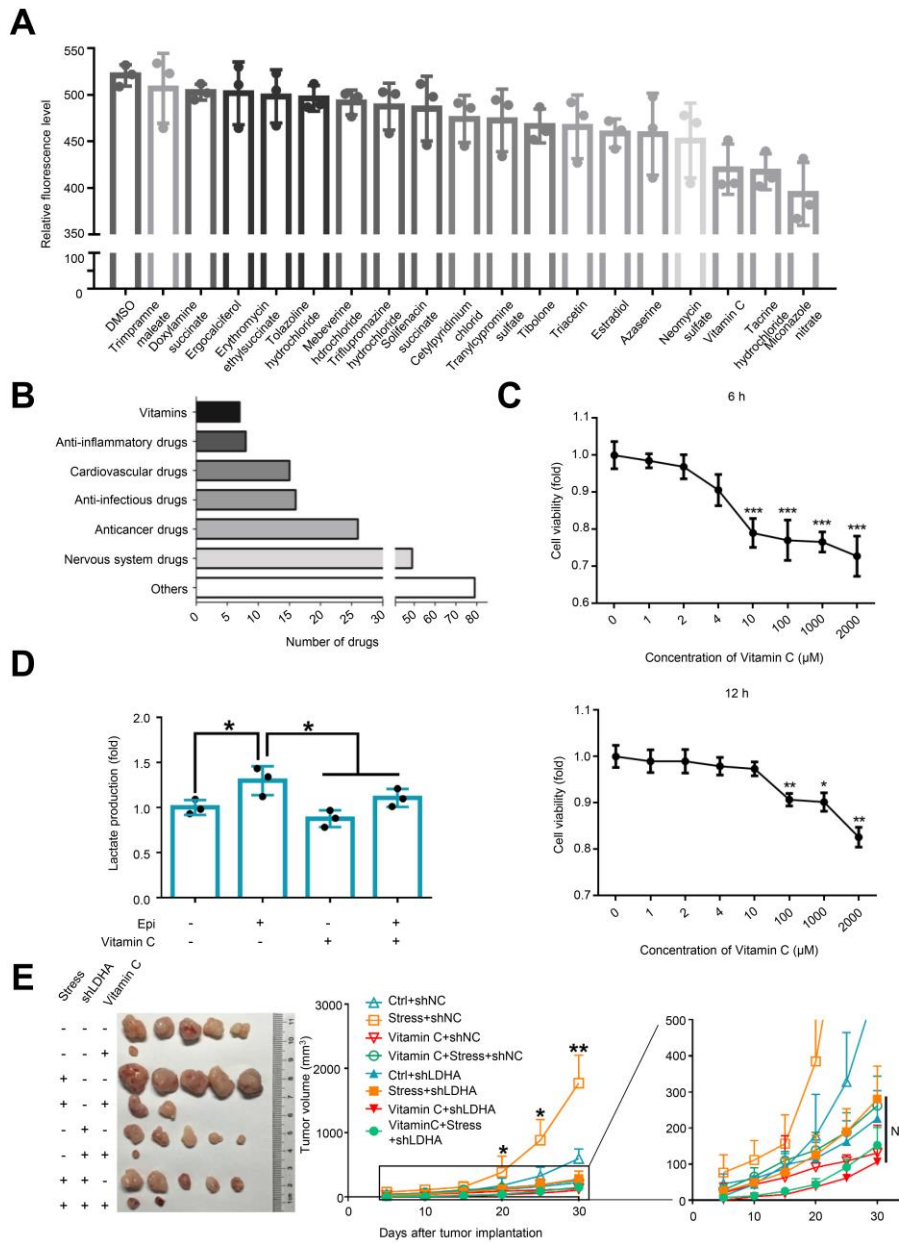
1
2 **Supplemental Figure 5. Epinephrine enhances USP28 signaling through LDHA.** (A) MDA-
3 MB-231 cells were treated with epinephrine for 5 days and OCR and ECAR were then measured.
4 n=3 (1-way ANOVA). (B) Average fold change of glycolytic metabolites was measured by
5 capillary electrophoresis-mass spectrometry. G-1-P, glucose-1-phosphate; 6-PG, 6-
6 phosphogluconic acid. n=3 (Student's t test). (C) MCF-7 cells were treated with PBS or Epi for 5
7 days and cell lysates were subjected to immunoblot analysis to quantify selected proteins. (D)
8 Immunoblot analysis with indicated antibodies in MDA-MB-231 cells treated with NE or Cort
9 (10 μM). (E) MDA-MB-231 and MCF-7 cells were maintained in low- (1 g/l) or high-glucose
10 (4.5 g/l) and cell lysates were subjected to immunoblot analysis to detect the indicated proteins.
11 (F) MCF-7 cells were transfected with HK2 siRNA in the presence or absence of Epi for 5 days.
12 Cell lysates were immunoblotted with antibodies against the indicated proteins. Data are
13 representative of at least 3 independent experiments. Data represent mean ± SEM, *p < 0.05, **p
14 < 0.01.



1
2 **Supplemental Figure 6. Epinephrine stabilizes USP28 through LDHA.** (A) MDA-MB-231
3 and MCF-7 cells were transfected with shLDHA or oeLDHA in the presence or absence of Epi
4 for 5 days. USP28 mRNA were examined by RT-qPCR. n=3 (1-way ANOVA). (B) MCF-7 cells
5 were treated with the indicated concentrations of sodium oxamate (Oxa) for 48h and expression
6 of the indicated proteins was examined by immunoblotting. (C) MDA-MB-231 cells were treated
7 with lactate (Lac) for 72 h. After treating the cells with CHX for the indicated times, expression
8 of USP28 was analyzed by immunoblotting (left panel). Intensity of USP28 expression for each
9 time point was quantified by densitometry and plotted against time (right panel). Half-life ($T_{1/2}$,
10 min) of USP28 following PBS was 25 min and for Epi it was 37 min in MDA-MB-231 cells. (D)
11 293T cells were transfected with USP28 WT or C171A and then treated with lactate for 72 h.
12 Extracts were immunoprecipitated with a MYC antibody and probed for expression of USP28
13 and MYC. (E) The distribution frequency for the distance of MYC^{Lys51} to USP28^{C171-H600} in
14 different pH conditions computed by constant pH molecular dynamics (CpHMD) simulation
15 method. Data are representative of at least 3 independent experiments. Data represent mean \pm
16 SEM.



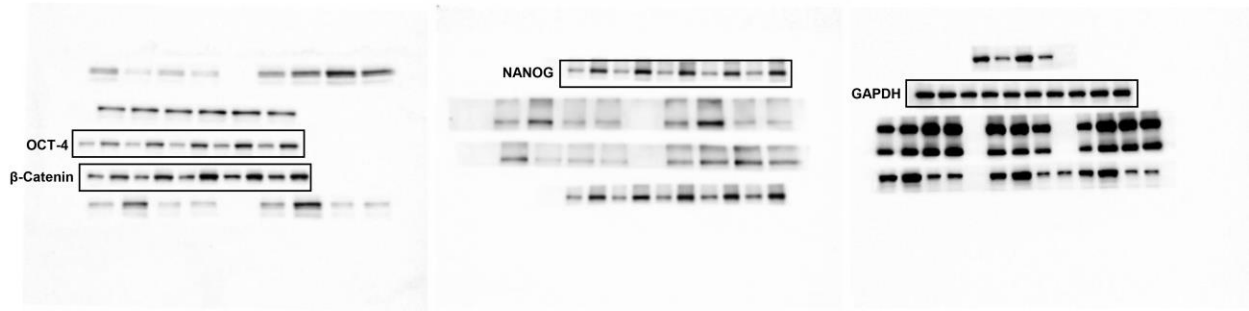
1
2 **Supplemental Figure 7. Chronic stress is related to poor clinical outcome in patients with**
3 **breast cancer.** (A) Receiver operating characteristic (ROC) curve of sensitivity versus
4 specificity of Epi^{high} (n=41) and Epi^{low} (n=42) groups. (B) Statistical analysis to determine the
5 correlation between serum Epi levels and LDHA, USP28, MYC and SLUG from the IHC
6 staining score in human breast cancer tissues. Epi^{high} (n=41) and Epi^{low} (n=42) (Student's *t* test).
7 (C) Relative fold-changes of selected proteins in patient tissues. n=5 (Student's *t* test). (D) ROC
8 curve of sensitivity versus specificity of LDHA^{high} (n=30) and LDHA^{low} (n=41) groups. Data are
9 representative of at least 3 independent experiments. Data represent mean ± SEM, ****p* < 0.001.



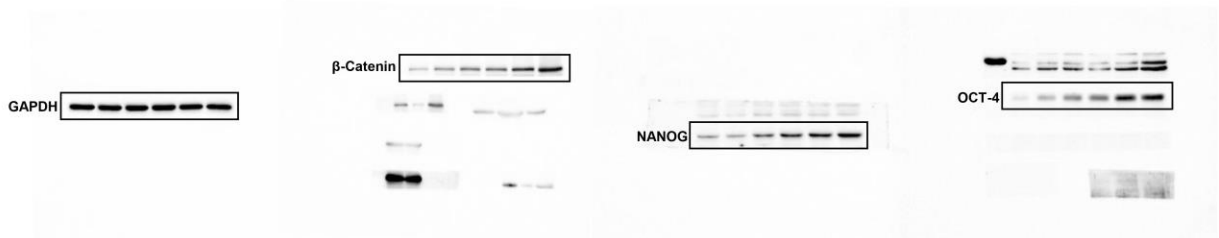
1
 2 **Supplemental Figure 8. Vitamin C is identified as the agent targeting LDHA.** (A) Relative
 3 fold-change of the top 18 drugs that showed a reduction in LDHA. (n=3) (B) The top 200 hits
 4 were classified into different groups according to drug indications or functions during the virtual
 5 screening of 2,037 FDA-approved drugs against LDHA. (C) Cell viability of MDA-MB-231
 6 cells treated with the indicated doses of vitamin C. n=3 (Student's *t* test). (D) Lactate was
 7 examined using cell culture medium from MCF-7 cells. n=3 (Student's *t* test). (E) Representative
 8 tumor images derived from treated mice (left panel) and tumor growth curves (right panel). n=5
 9 (1-way ANOVA). Data are representative of at least 3 independent experiments. Data represent
 10 mean \pm SEM, **p* < 0.05, ***p* < 0.01, ****p* < 0.001.
 11

1 **Supplemental Movie 1. MD simulation on USP28^{WT} complexed with MYC⁴⁶⁻⁷⁴ motif.**
2 USP28^{WT} was depicted in gray and MYC⁴⁶⁻⁷⁴ motif was shown in green. The Cys/Ala¹⁷¹
3 mutation site was displayed in red, and Lys⁵¹ and Lys⁵² in the MYC motif were depicted as blue
4 spheres. States were collected for 0–150 ns after each ns.
5
6 **Supplemental Movie 2. MD simulation for mutant USP28^{C171A} complexed with MYC⁴⁶⁻⁷⁴**
7 **motif.**
8 USP28^{C171A} was depicted in gray and MYC⁴⁶⁻⁷⁴ motif was shown in green. The Cys/Ala¹⁷¹
9 mutation site was displayed in red, and Lys⁵¹ and Lys⁵² in the MYC motif were depicted as blue
10 spheres. States were collected for 0–150 ns after each ns.
11
12 **Supplemental Movie 3. MD simulation of Vitamin C complexed in the pocket of LDHA.**
13 LDHA was depicted in gray, co-factor was depicted in stick model and vitamin C was depicted
14 in gold sphere model. States were collected for 0–50 ns after each ns.

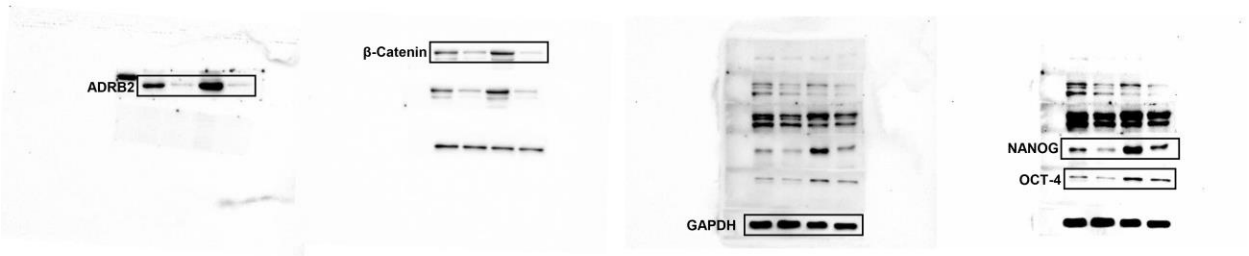
Full unedited gel for Figure 1B



Full unedited gel for Figure 1F

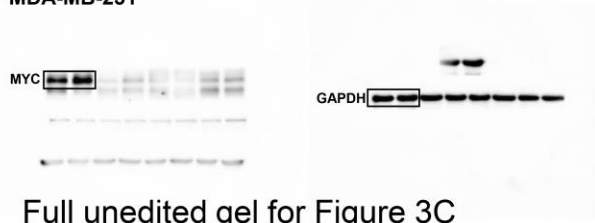


Full unedited gel for Figure 1H



Full unedited gel for Figure 3A

MDA-MB-231



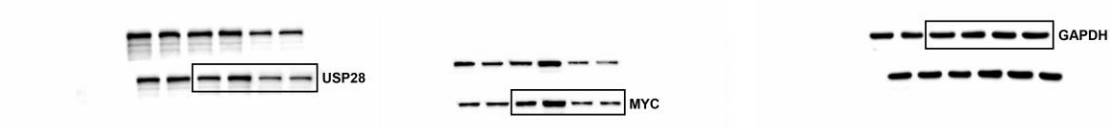
MCF-7



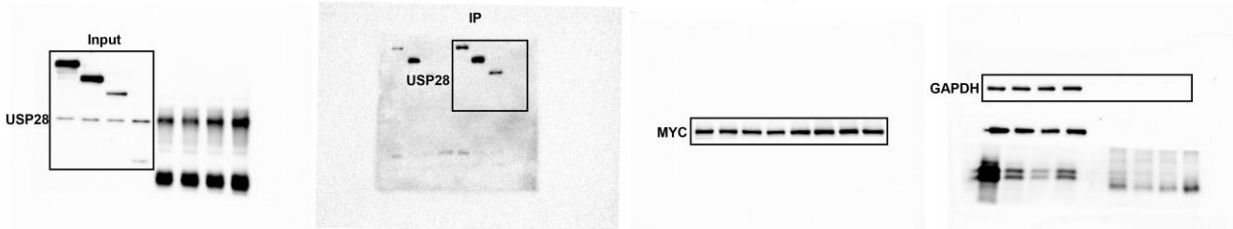
Full unedited gel for Figure 3C



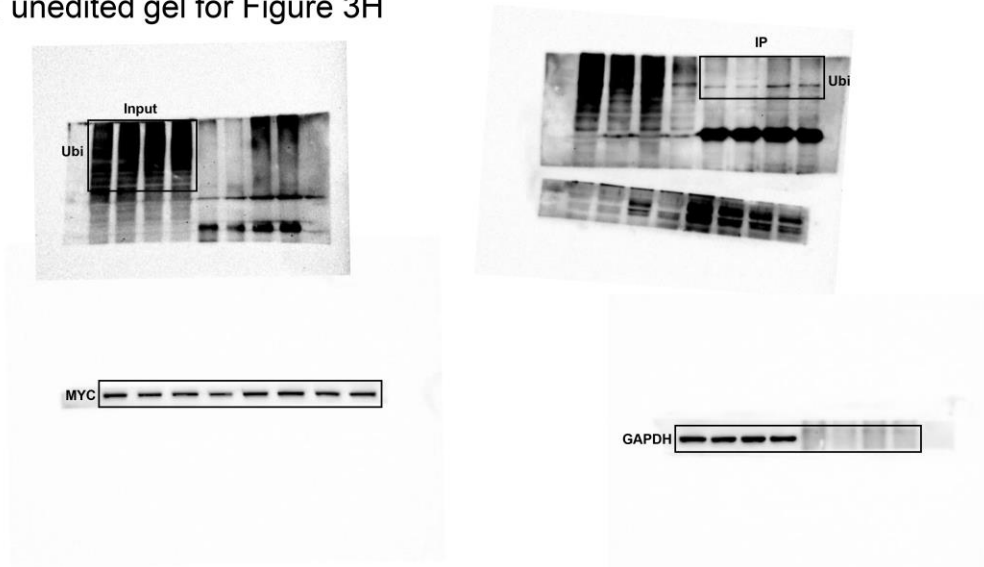
Full unedited gel for Figure 3E



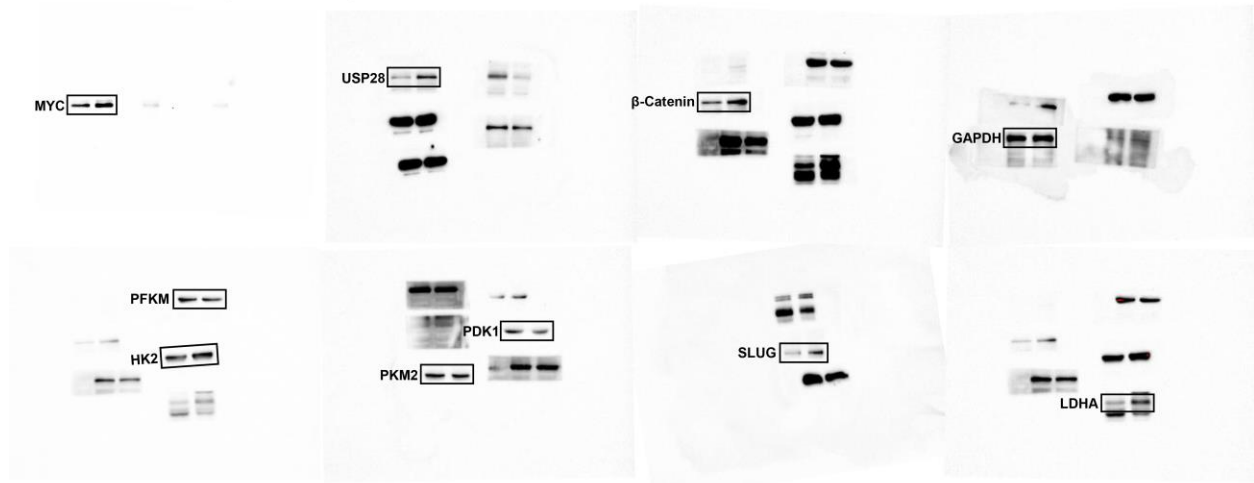
Full unedited gel for Figure 3F



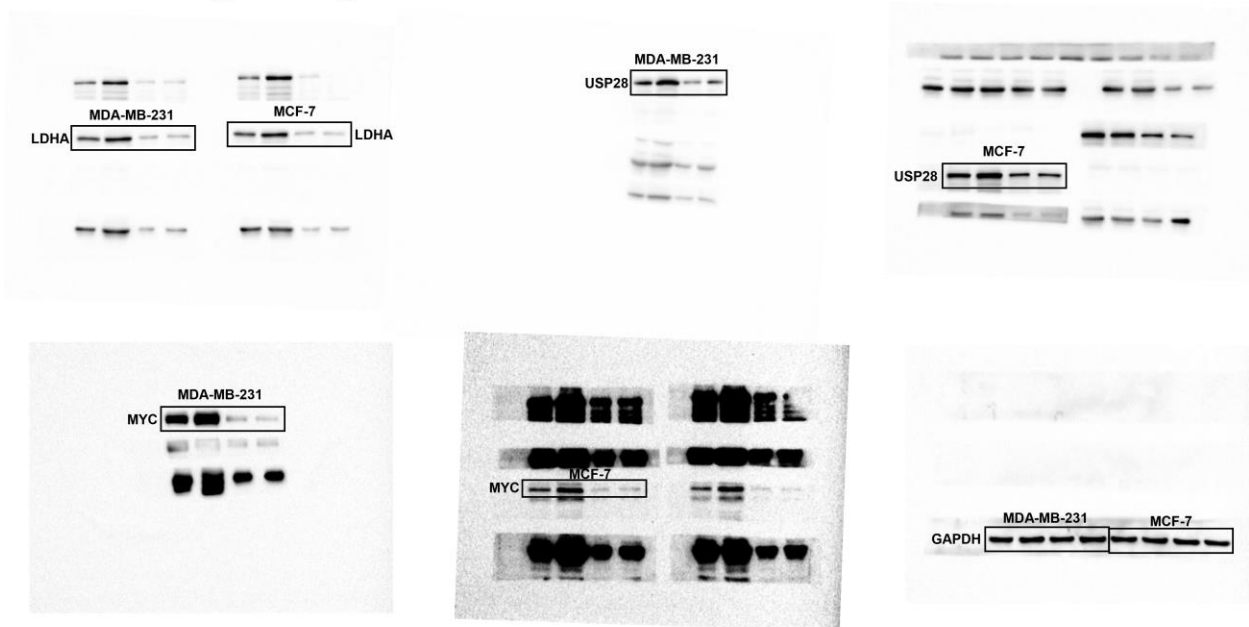
Full unedited gel for Figure 3H



Full unedited gel for Figure 4D



Full unedited gel for Figure 4E



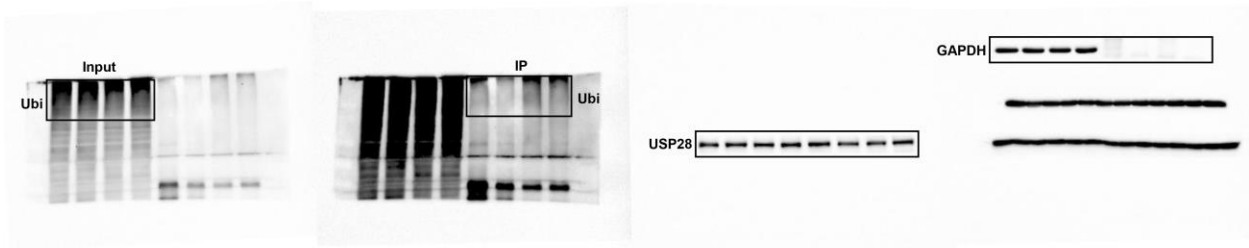
Full unedited gel for Figure 5A



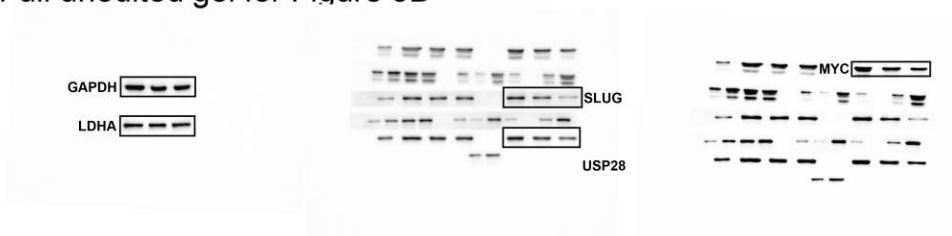
Full unedited gel for Figure 5B



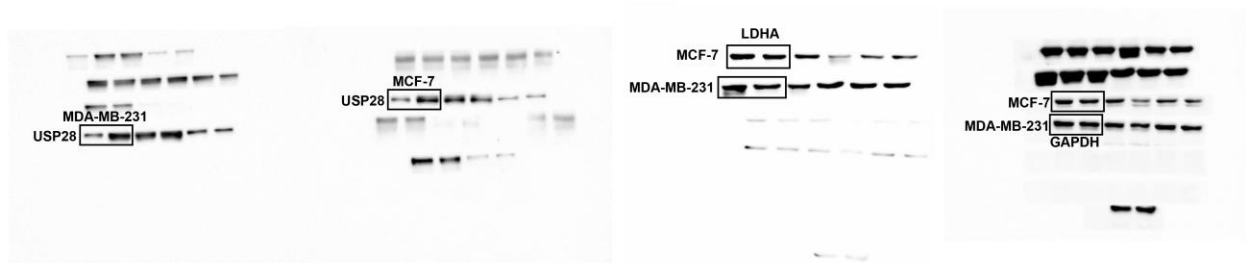
Full unedited gel for Figure 5C



Full unedited gel for Figure 5D



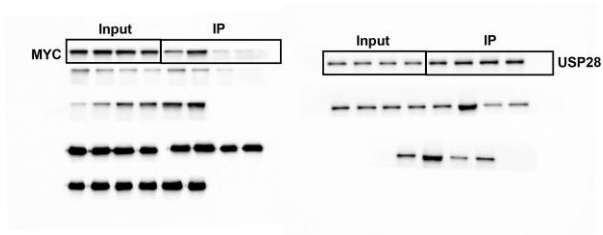
Full unedited gel for Figure 5E



Full unedited gel for Figure 5F



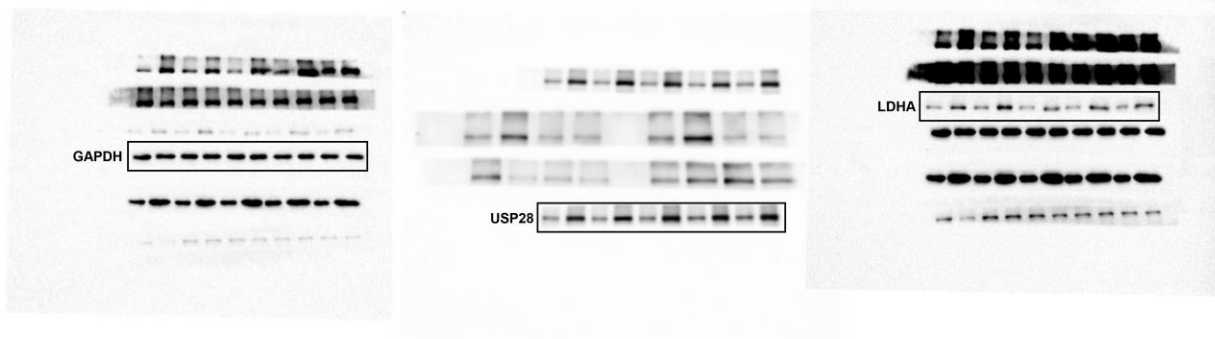
Full unedited gel for Figure 5G



Full unedited gel for Figure 5H

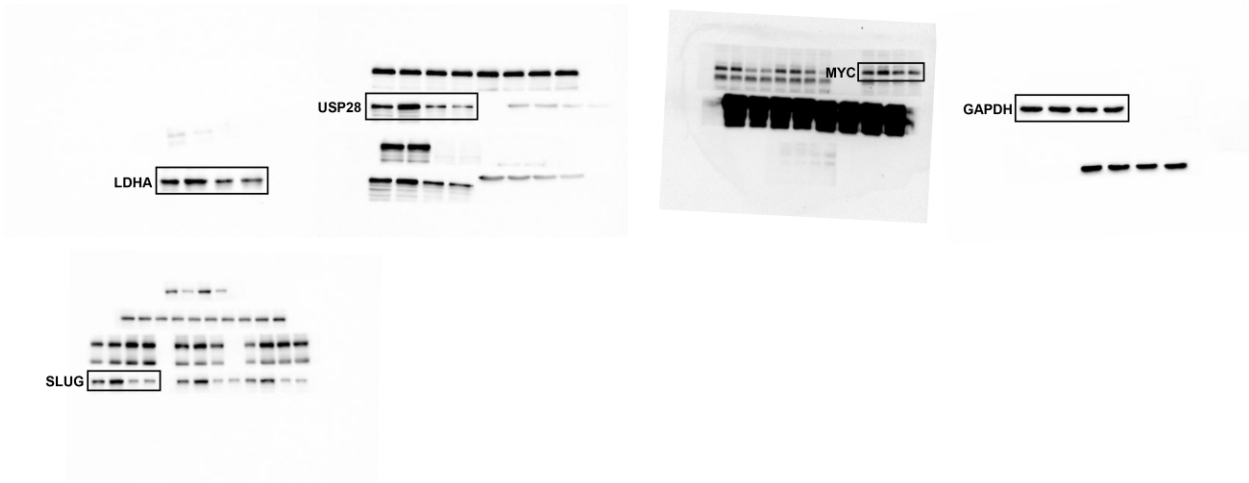


Full unedited gel for Figure 6B

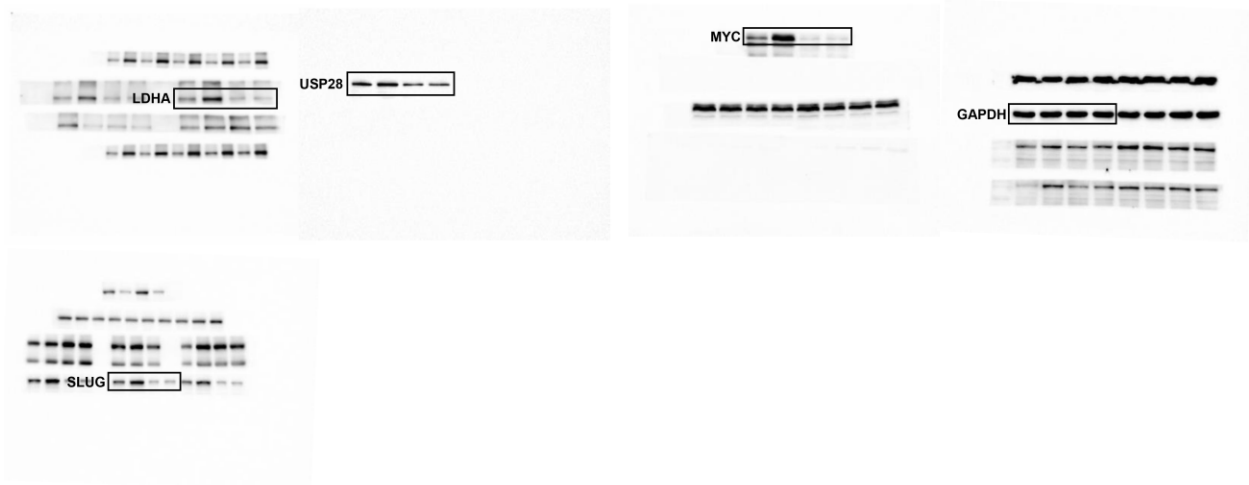


Full unedited gel for Figure 7C

MDA-MB-231



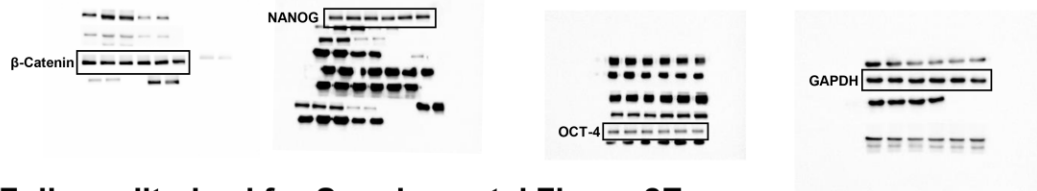
MCF-7



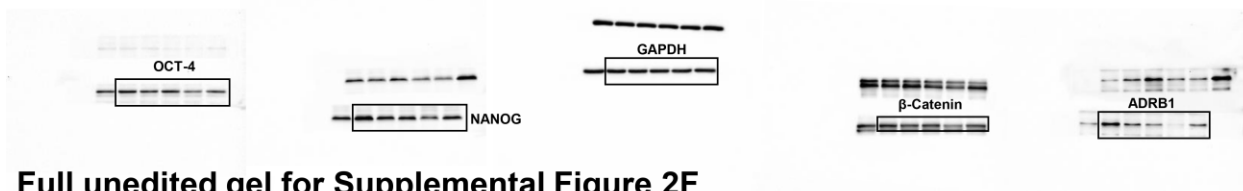
Full unedited gel for Supplemental Figure 2C



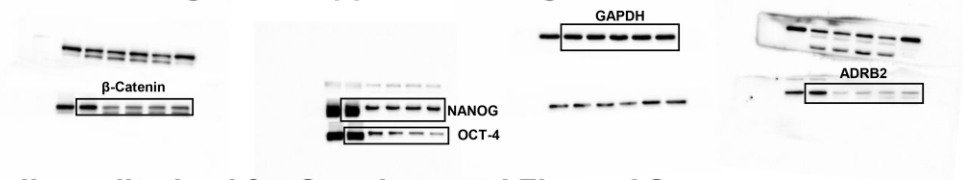
Full unedited gel for Supplemental Figure 2D



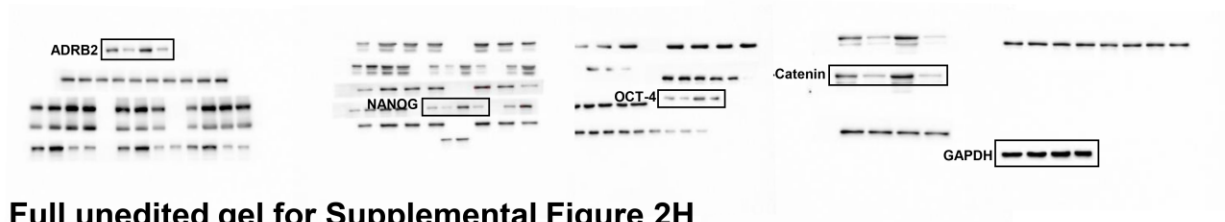
Full unedited gel for Supplemental Figure 2E



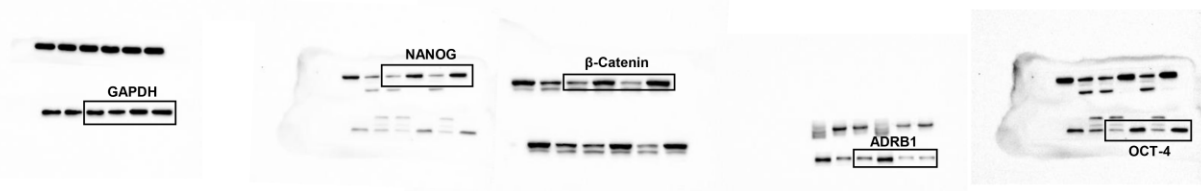
Full unedited gel for Supplemental Figure 2F



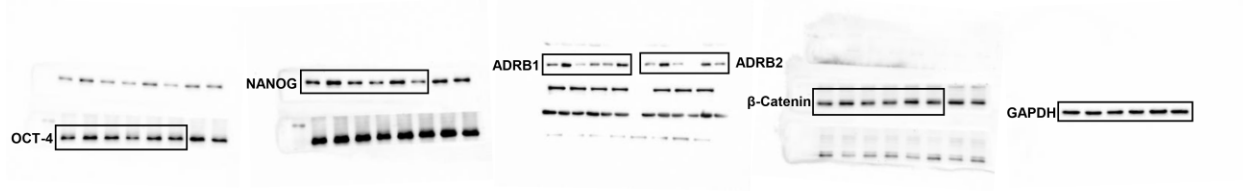
Full unedited gel for Supplemental Figure 2G



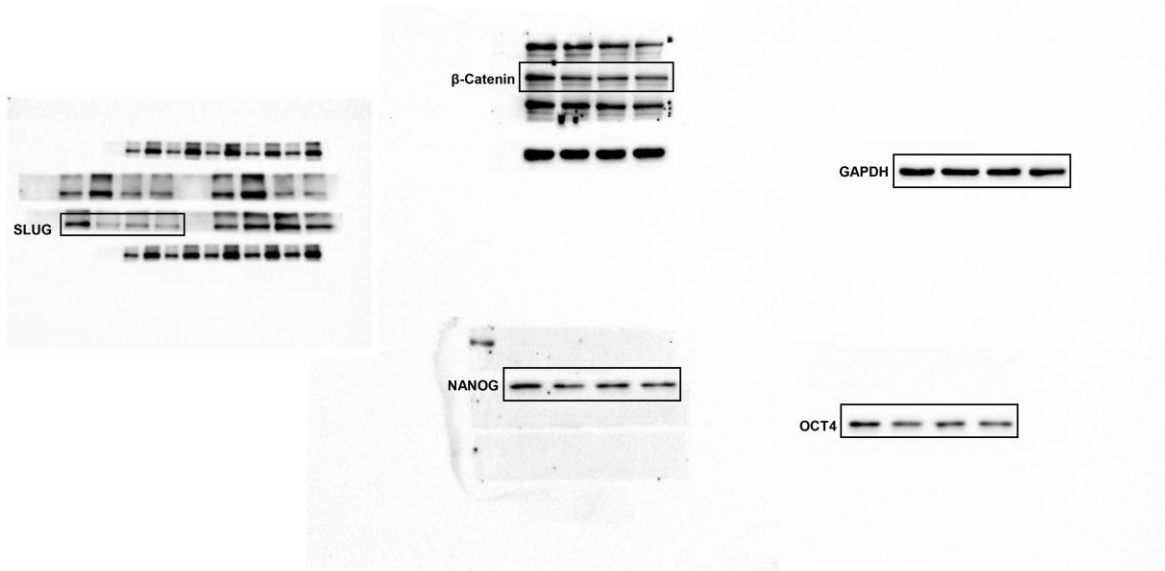
Full unedited gel for Supplemental Figure 2H



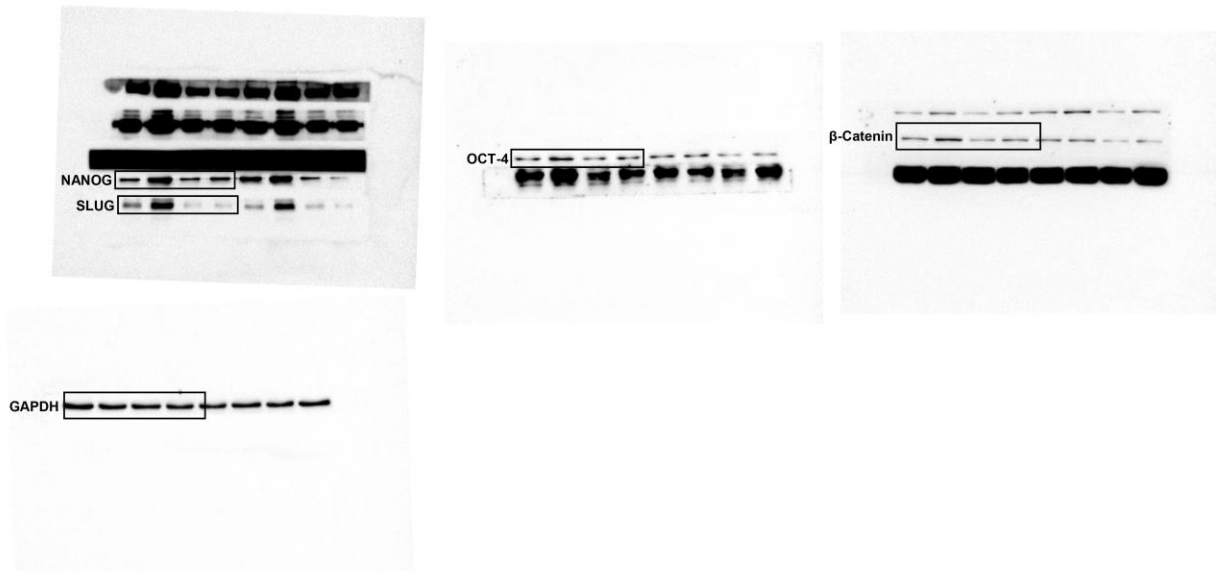
Full unedited gel for Supplemental Figure 2I



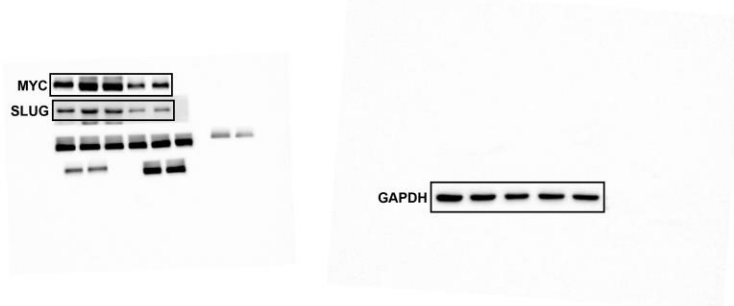
Full unedited gel for Supplemental Figure 3B



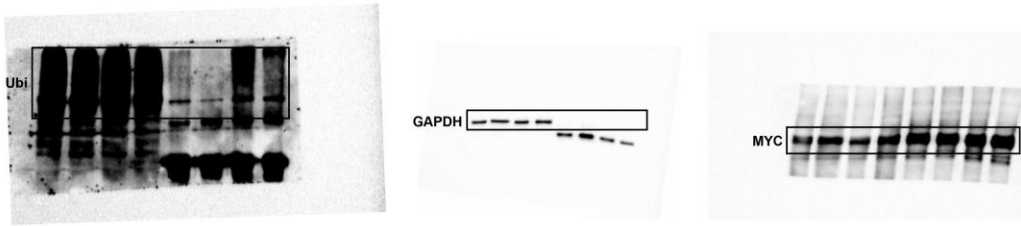
Full unedited gel for Supplemental Figure 3D



Full unedited gel for Supplemental Figure 3H



Full unedited gel for Supplemental Figure 4F



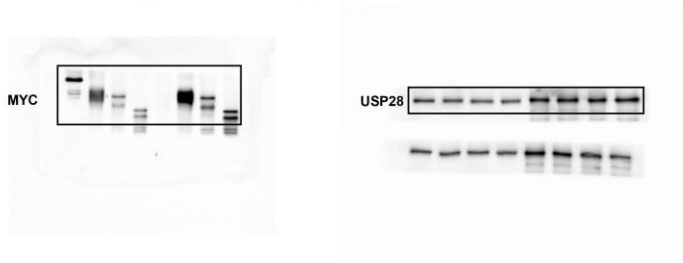
Full unedited gel for Supplemental Figure 4G



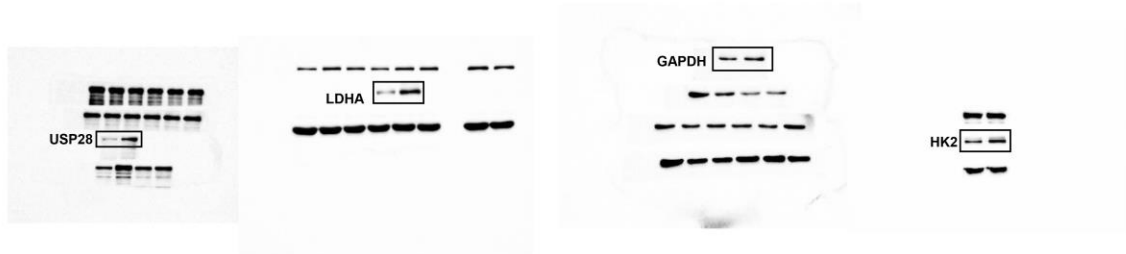
Full unedited gel for Supplemental Figure 4J



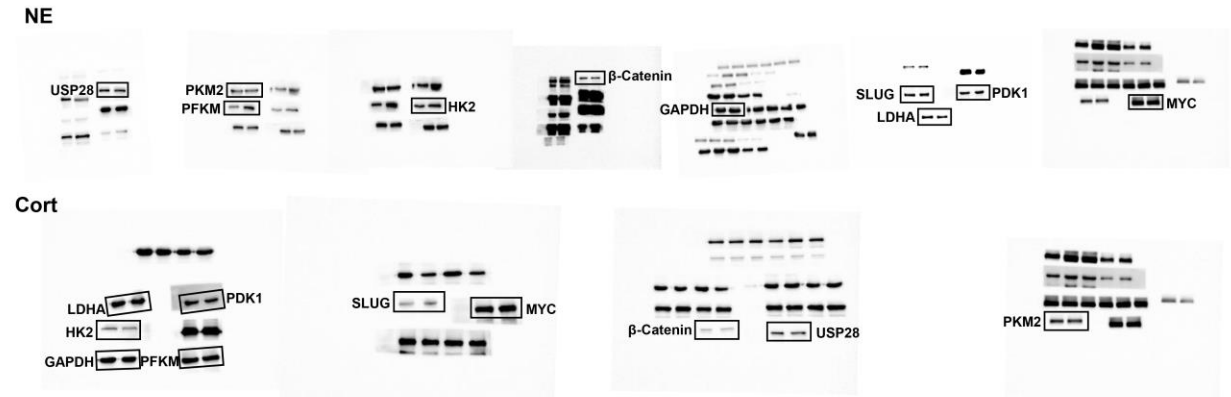
Full unedited gel for Supplemental Figure 4K



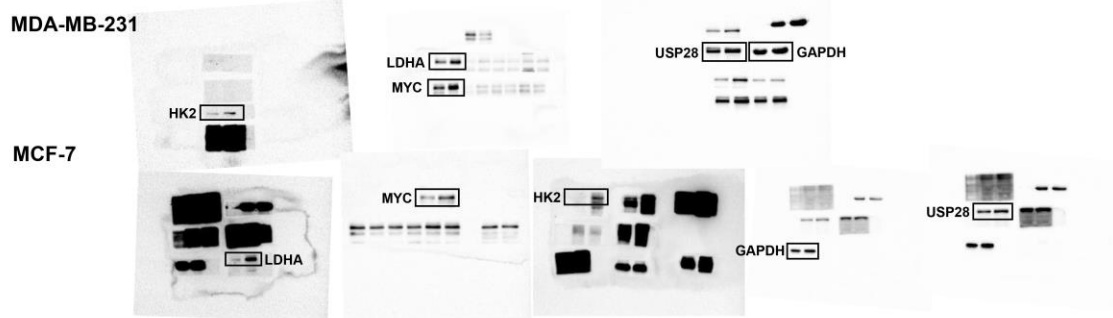
Full unedited gel for Supplemental Figure 5C



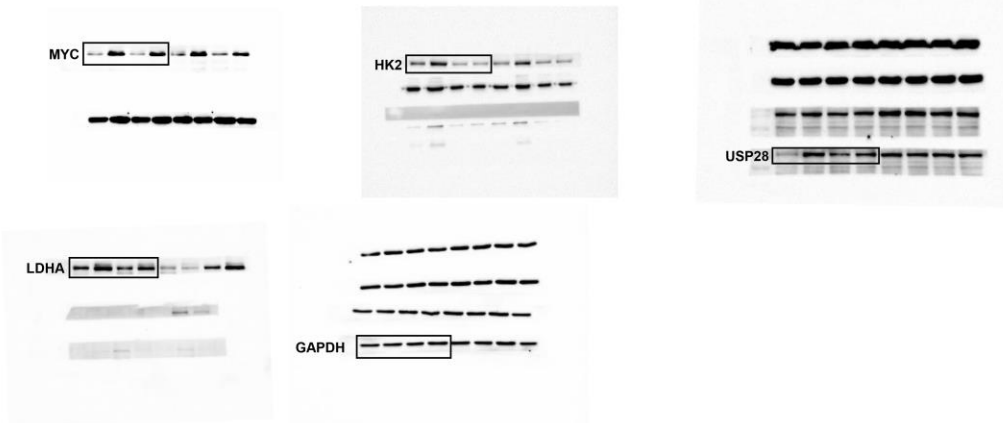
Full unedited gel for Supplemental Figure 5D



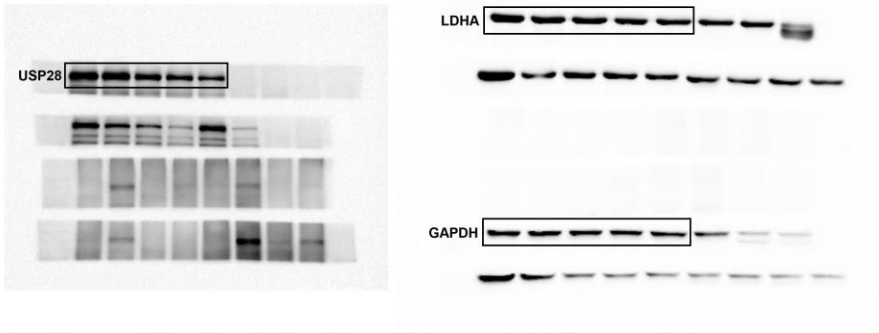
Full unedited gel for Supplemental Figure 5E



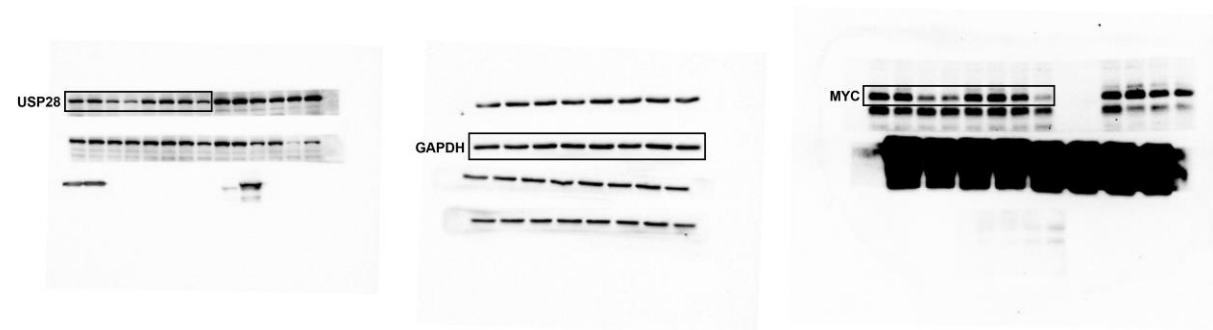
Full unedited gel for Supplemental Figure 5F



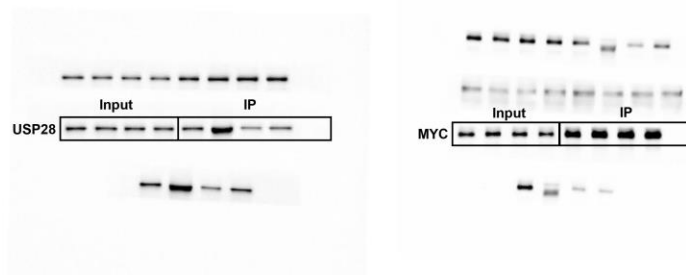
Full unedited gel for Supplemental Figure 6B

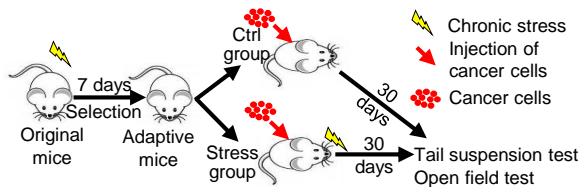
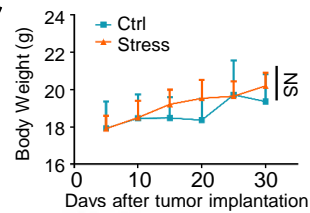
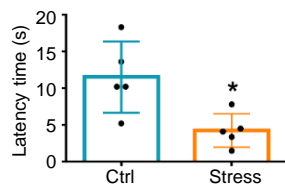
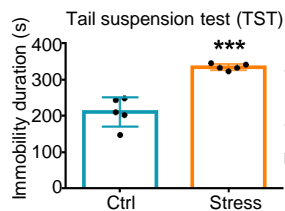
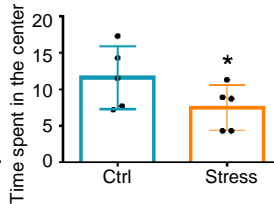
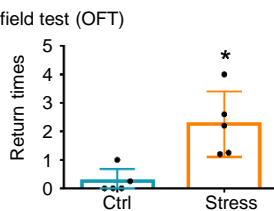
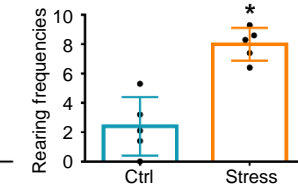
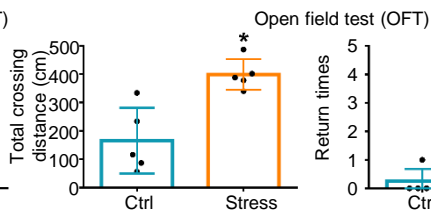
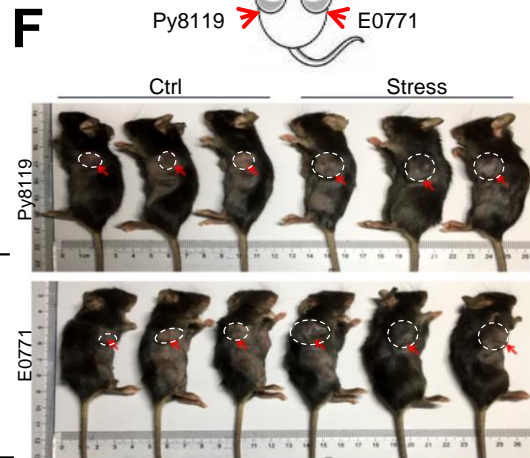
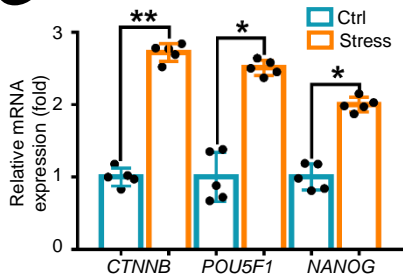
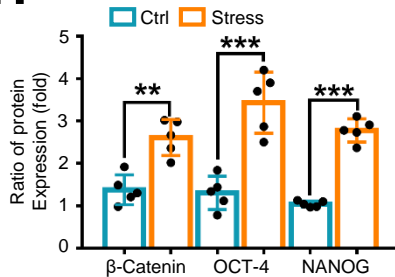
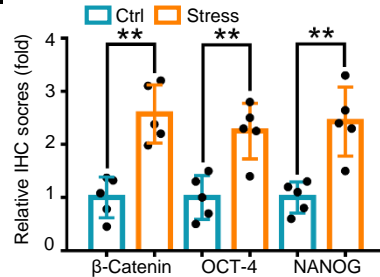
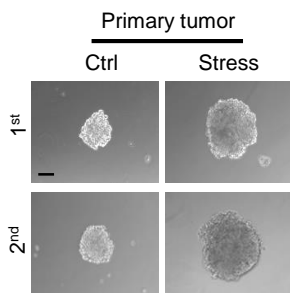
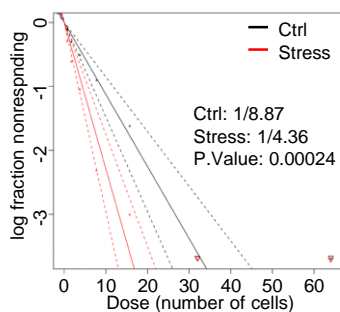
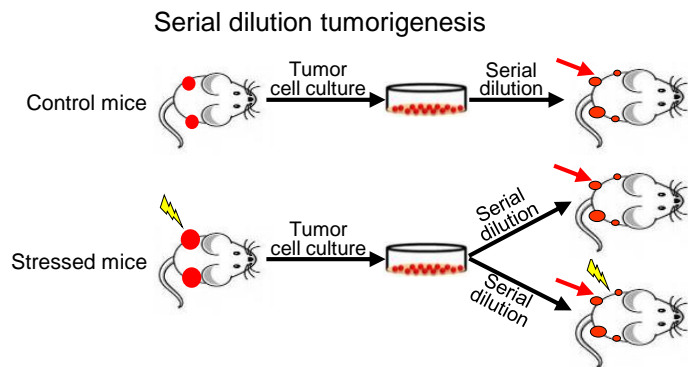


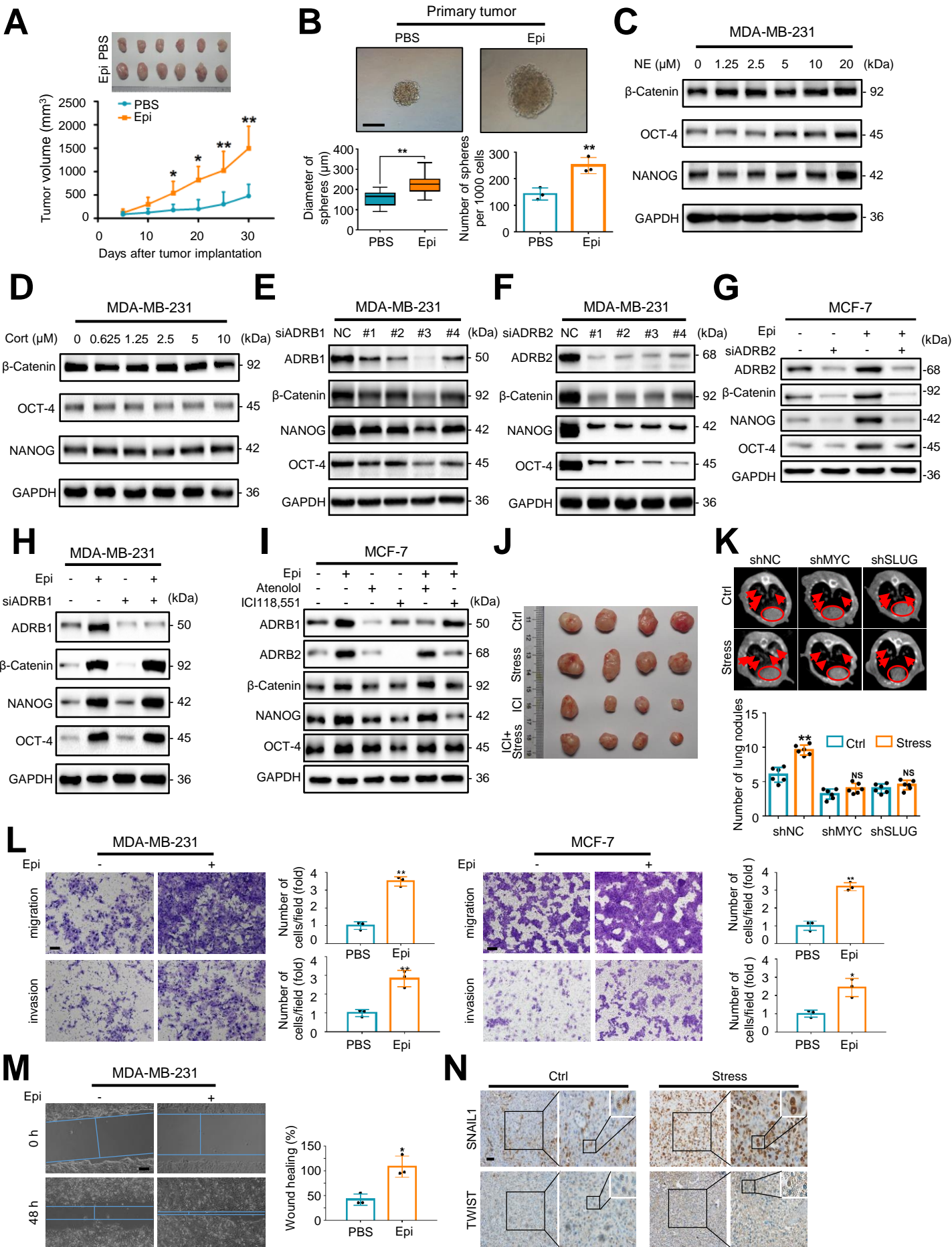
Full unedited gel for Supplemental Figure 6C

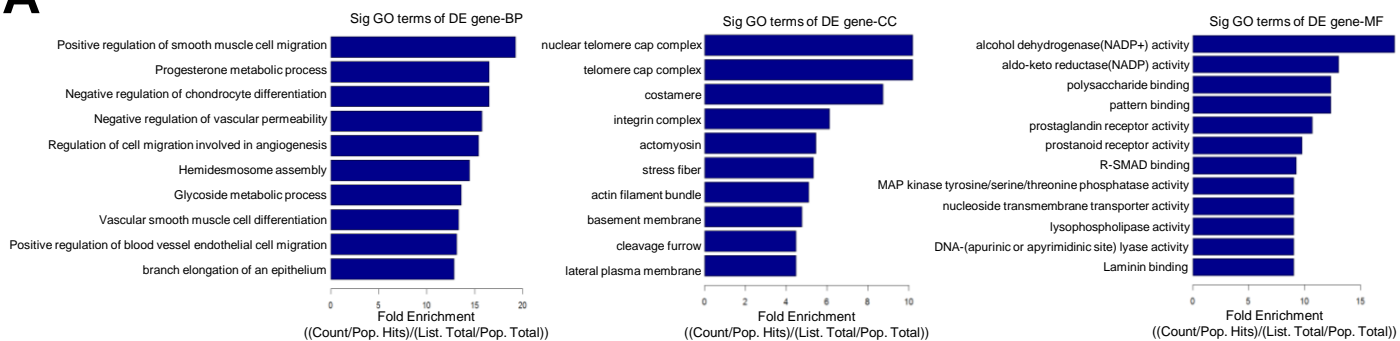
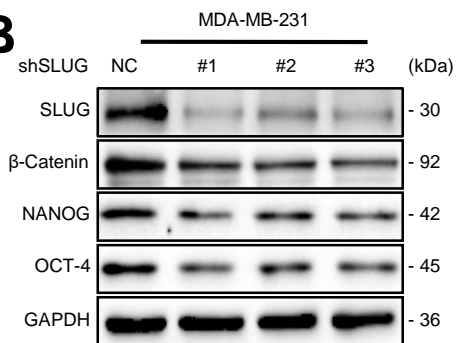
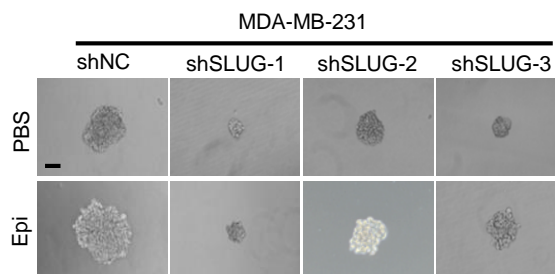
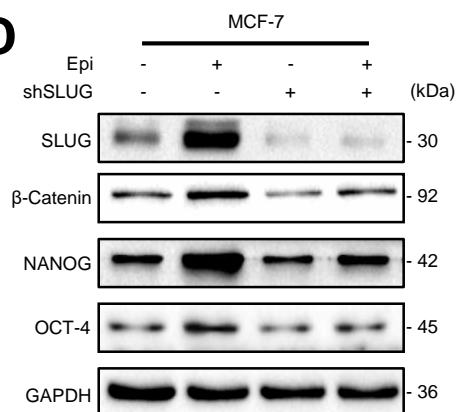
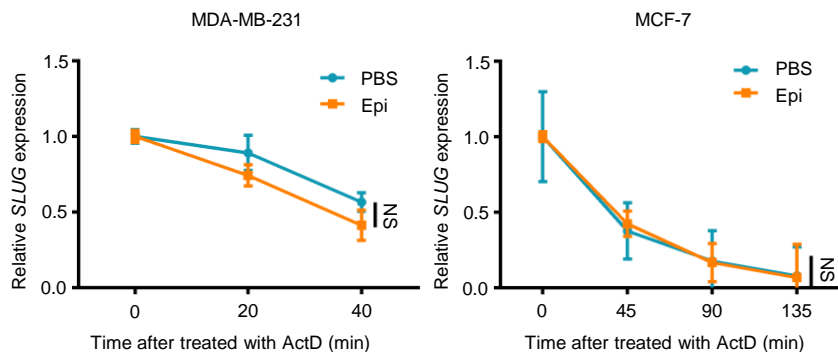
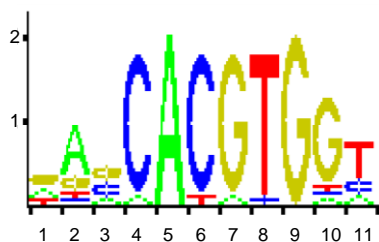
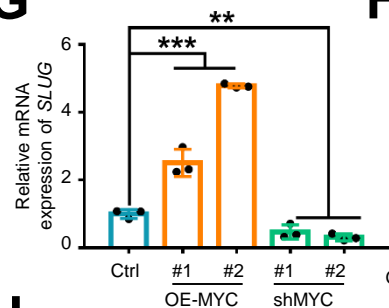
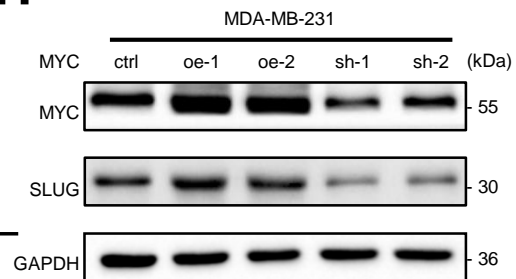
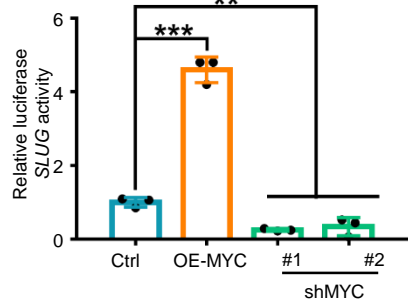
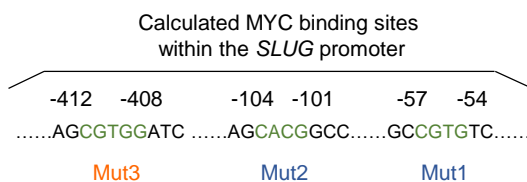


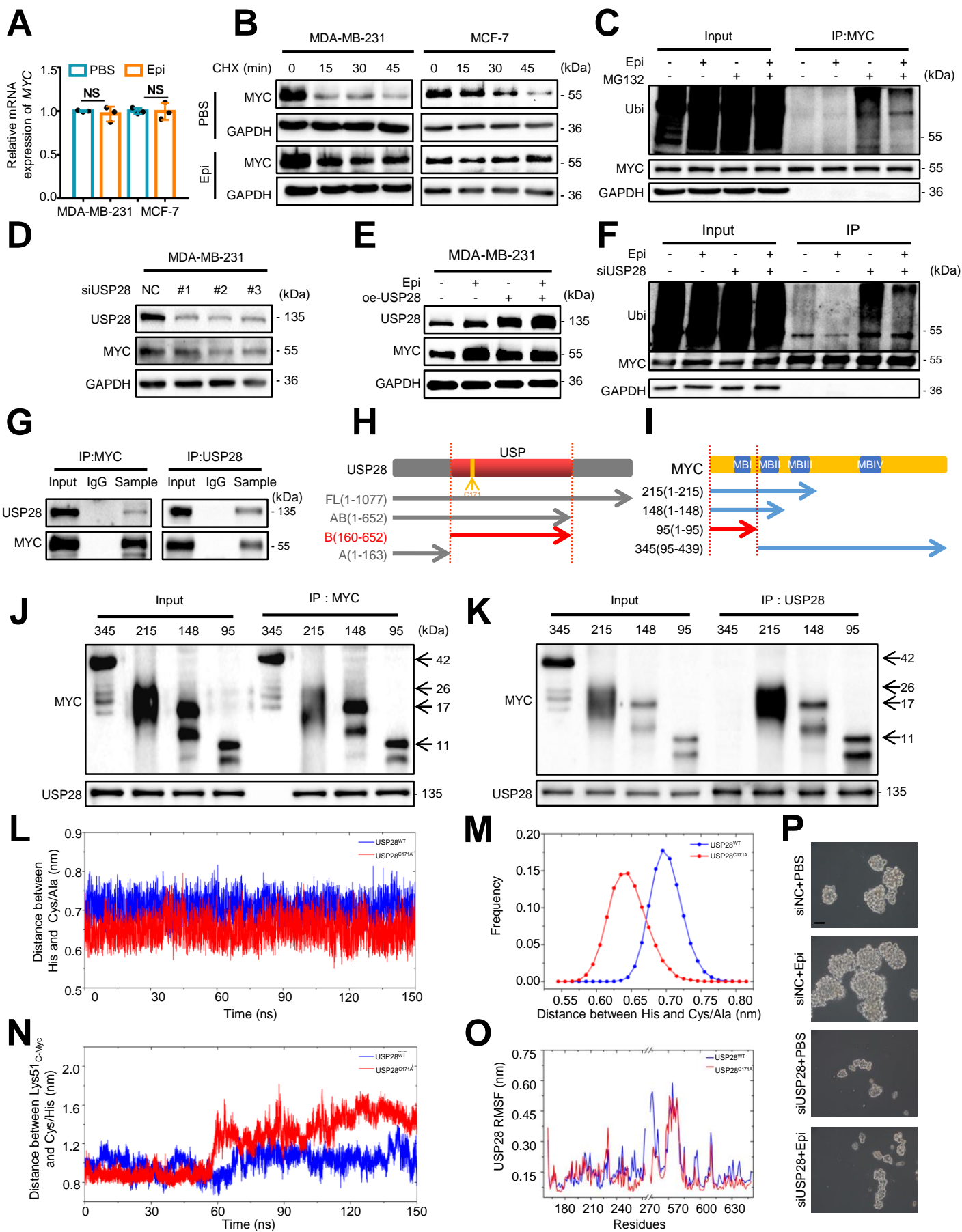
Full unedited gel for Supplemental Figure 6D

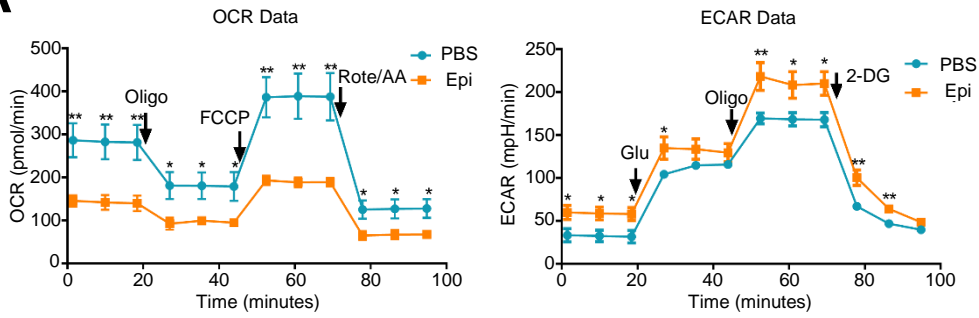
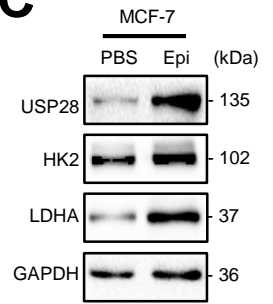
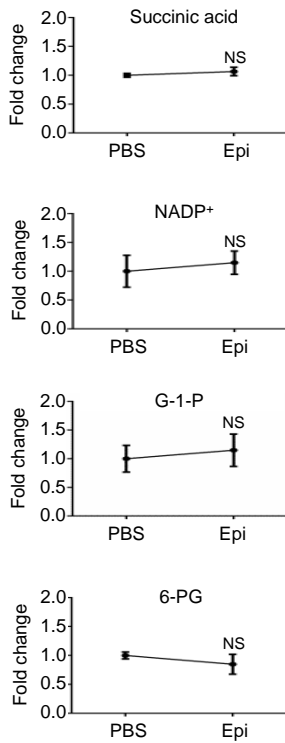
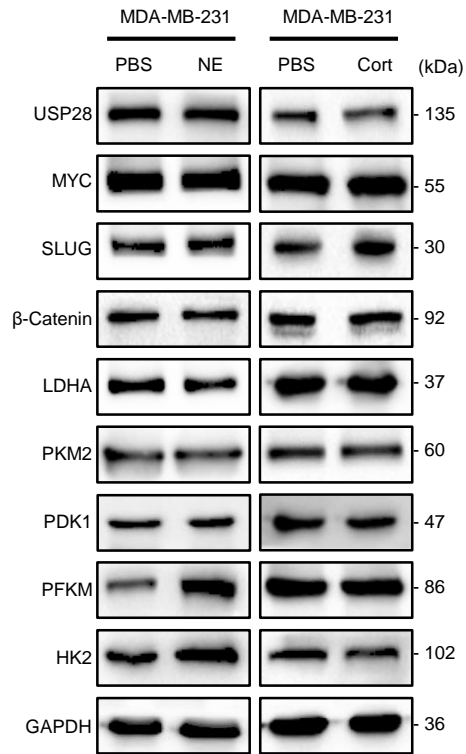
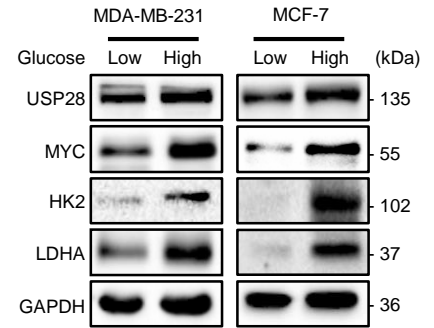
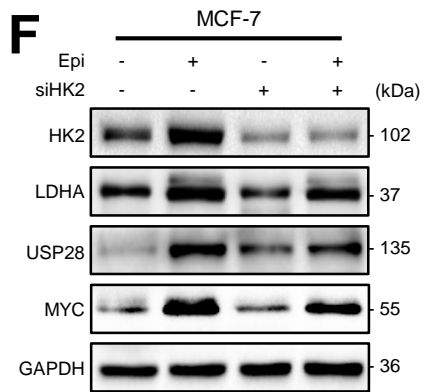


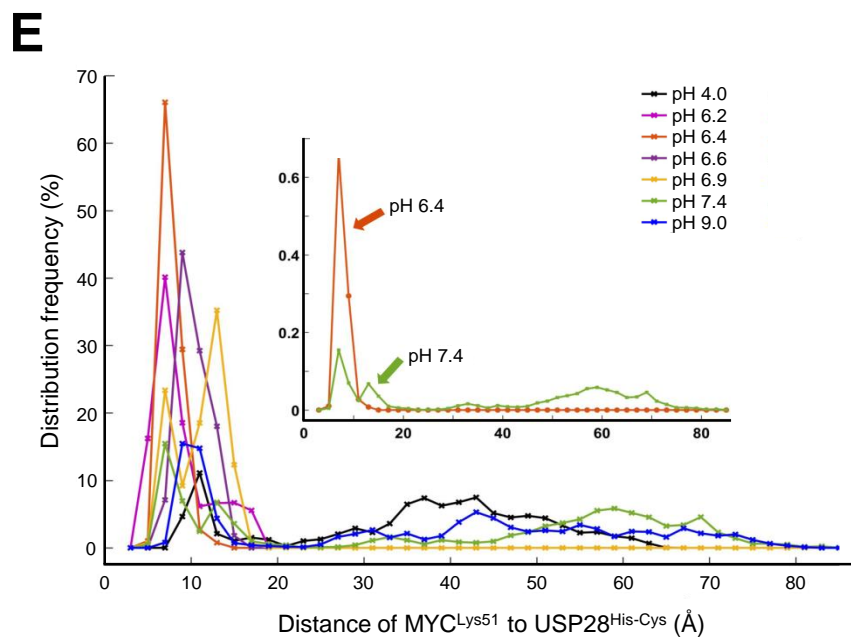
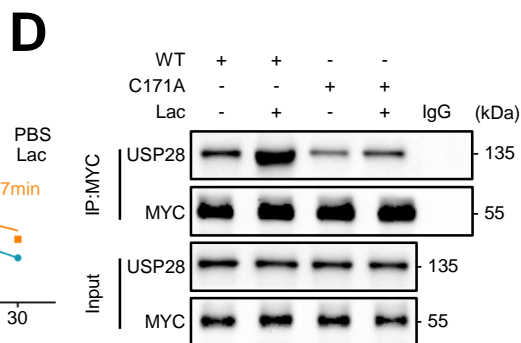
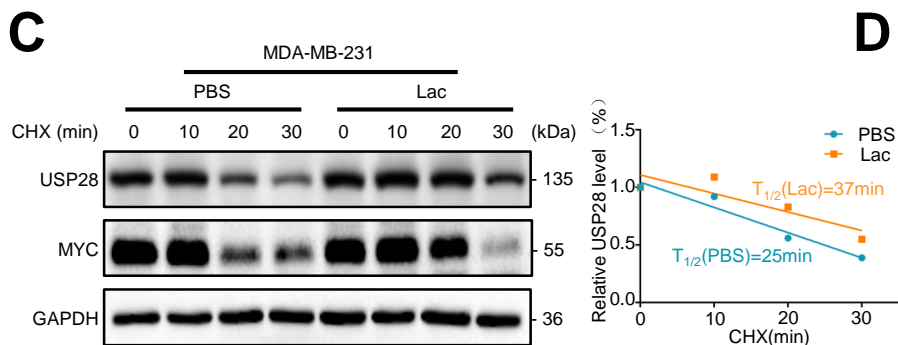
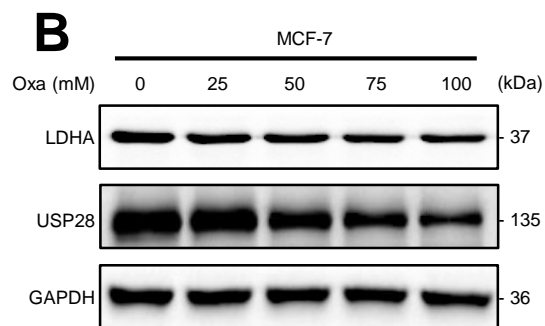
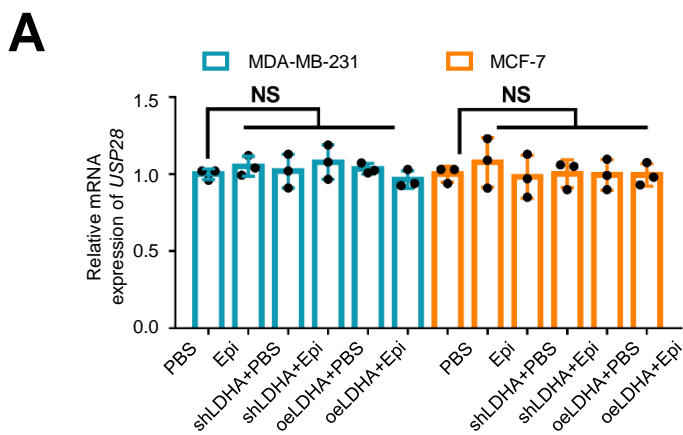
A**B****C****D****E****F****G****H****I****J****K****L**

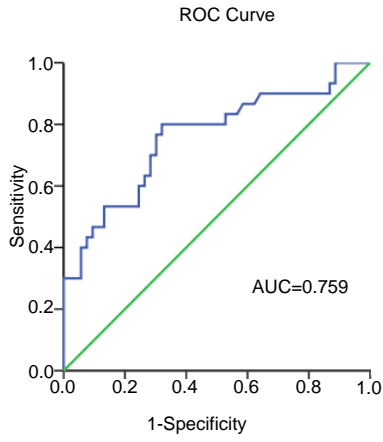
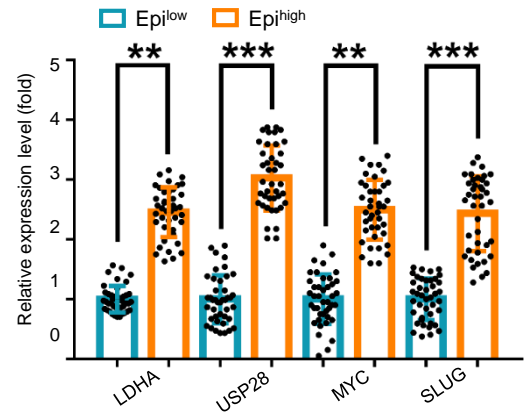
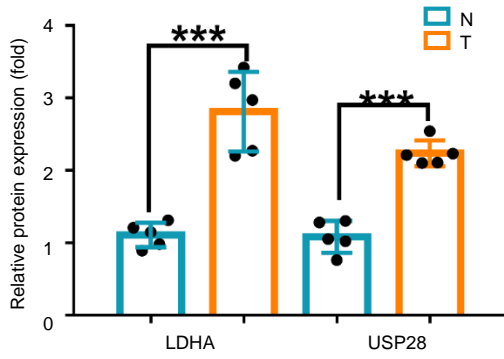
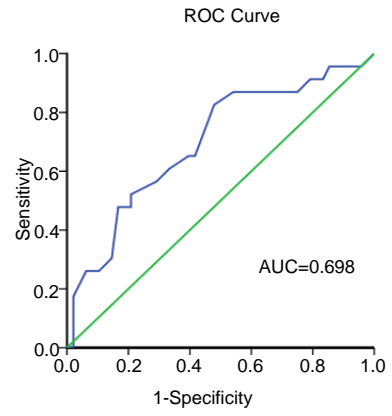


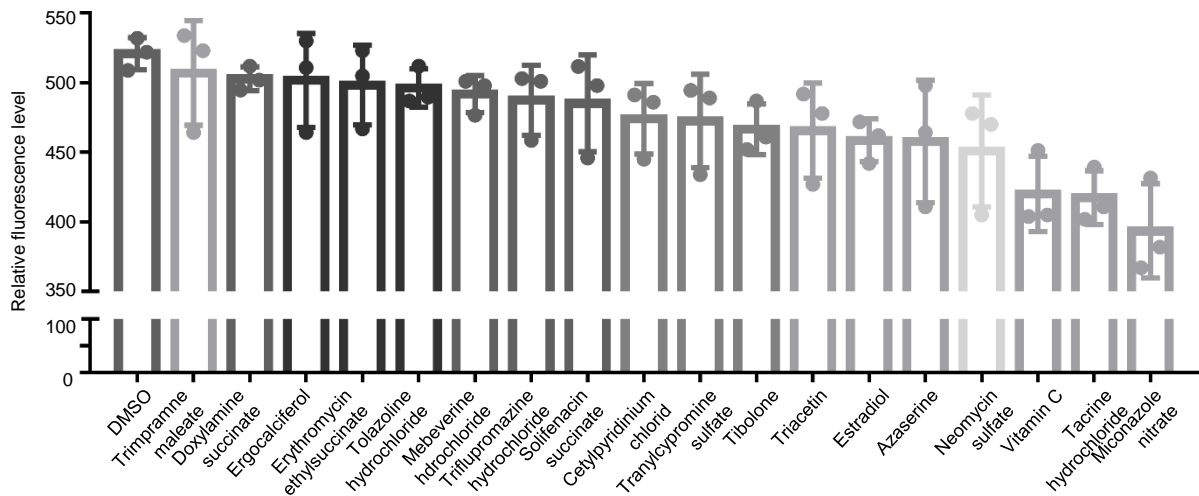
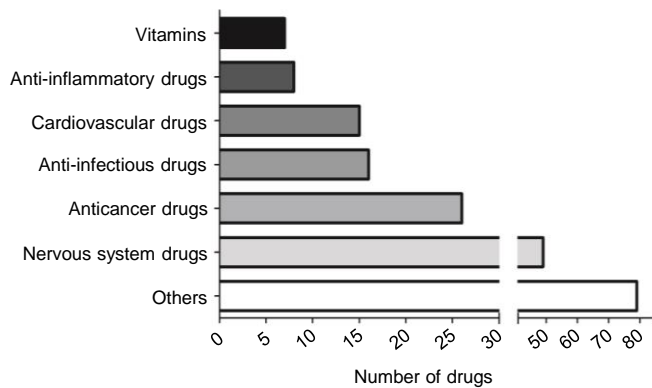
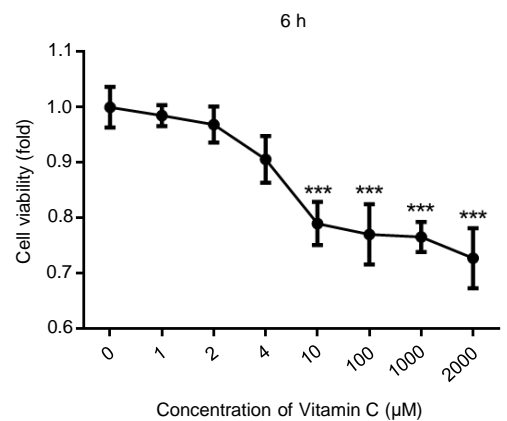
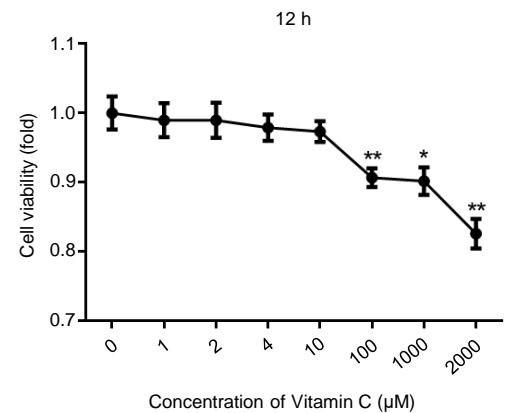
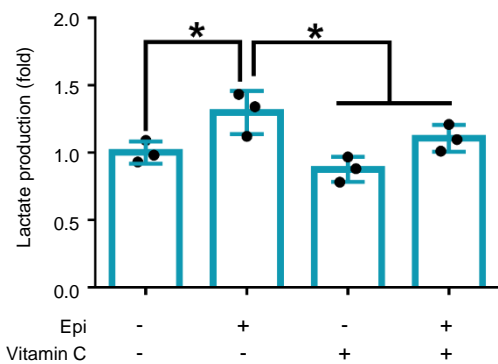
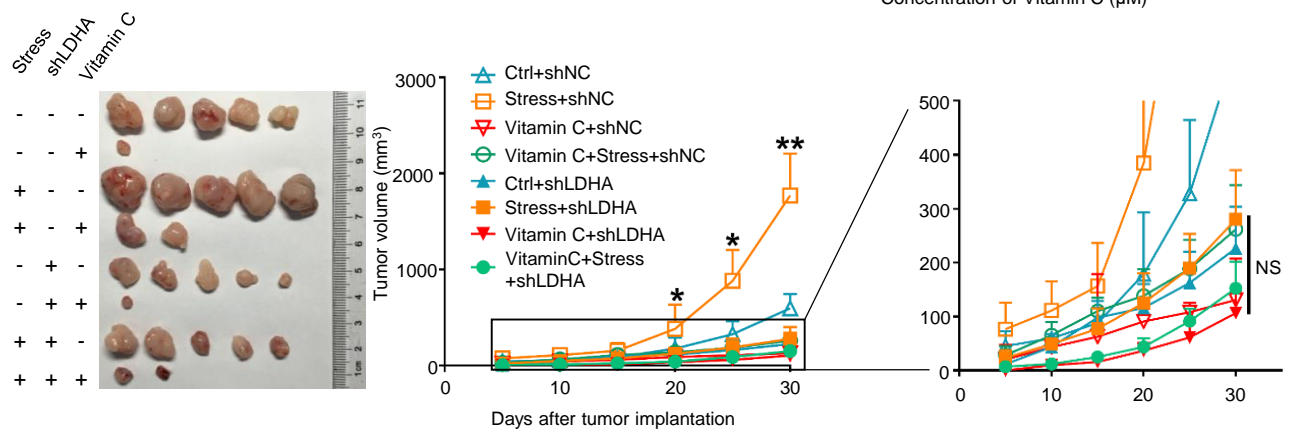
A**B****C****D****E****F****G****H****I****J**



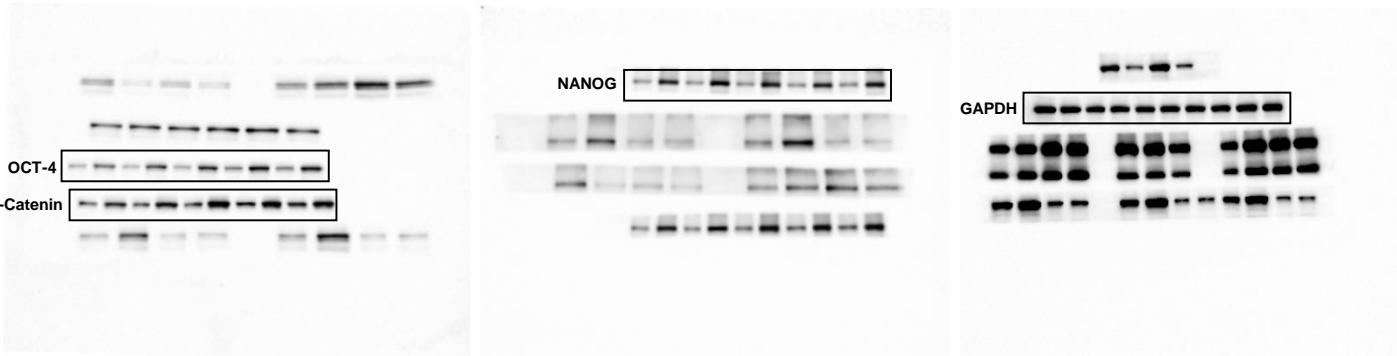
A**C****B****D****E****F**



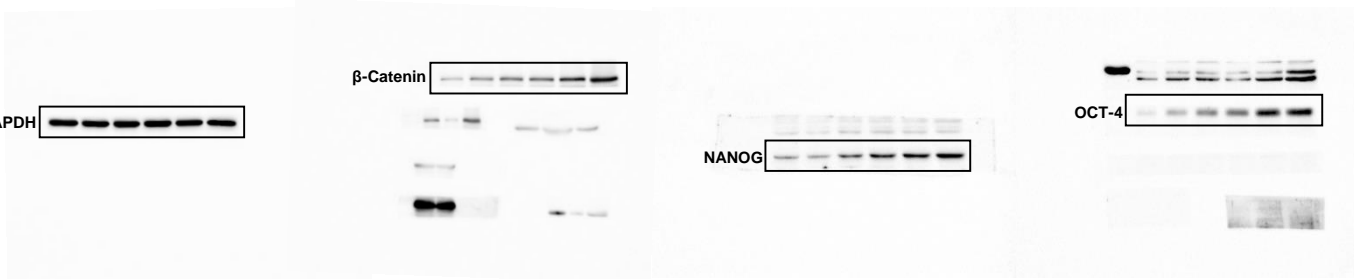
A**B****C****D**

A**B****C****D****E**

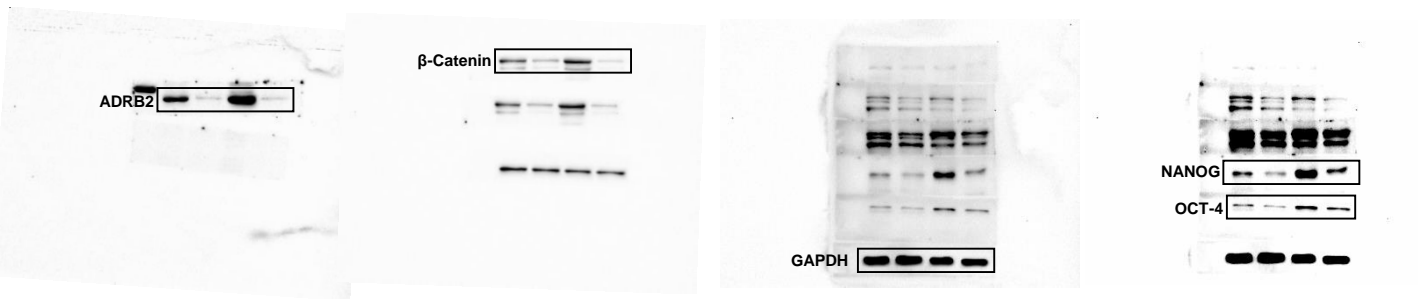
Full unedited gel for Figure 1B



Full unedited gel for Figure 1F

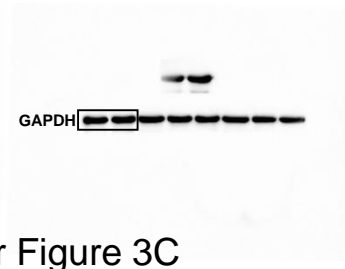
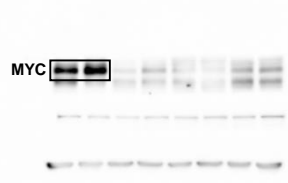


Full unedited gel for Figure 1H

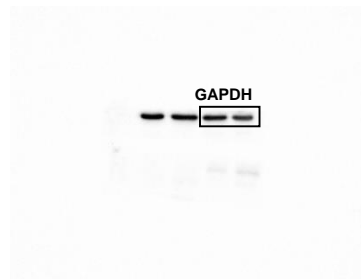


Full unedited gel for Figure 3A

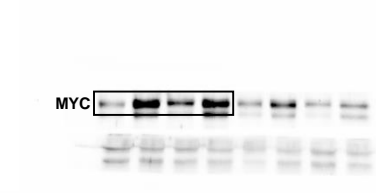
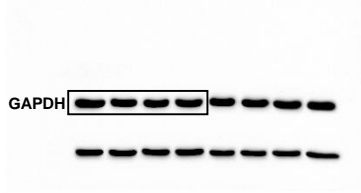
MDA-MB-231



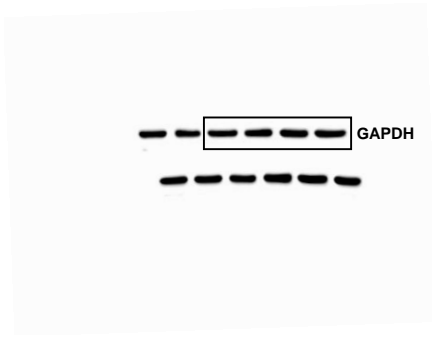
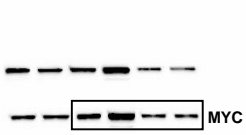
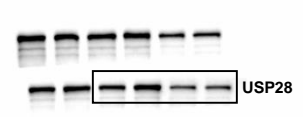
MCF-7



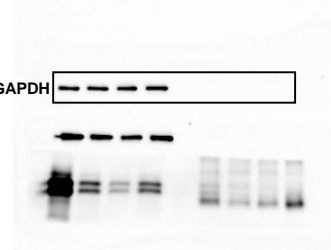
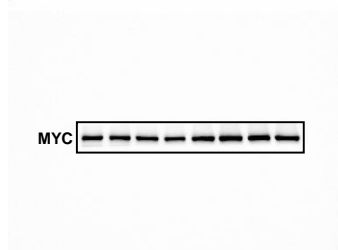
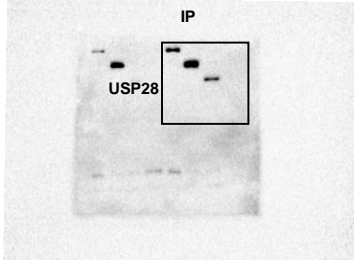
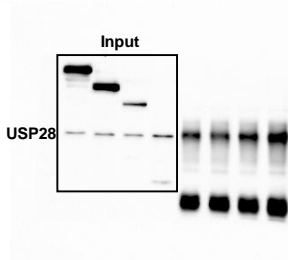
Full unedited gel for Figure 3C



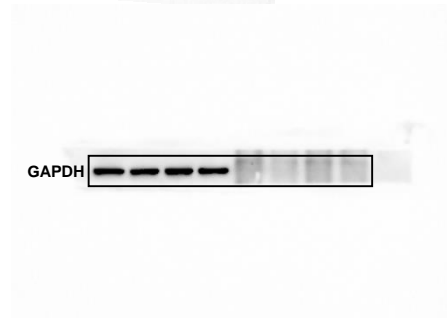
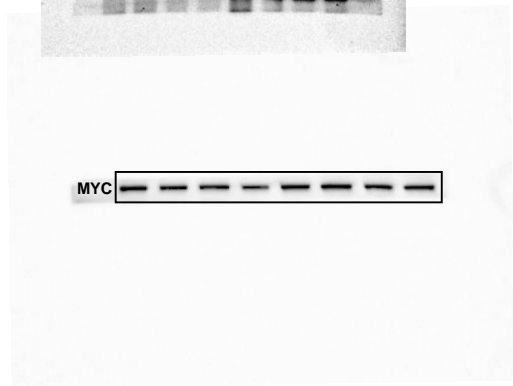
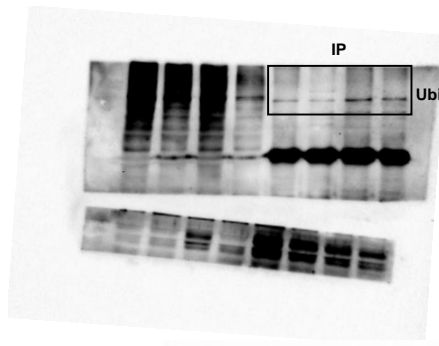
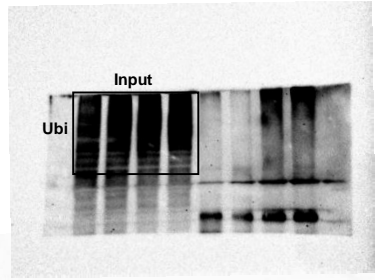
Full unedited gel for Figure 3E



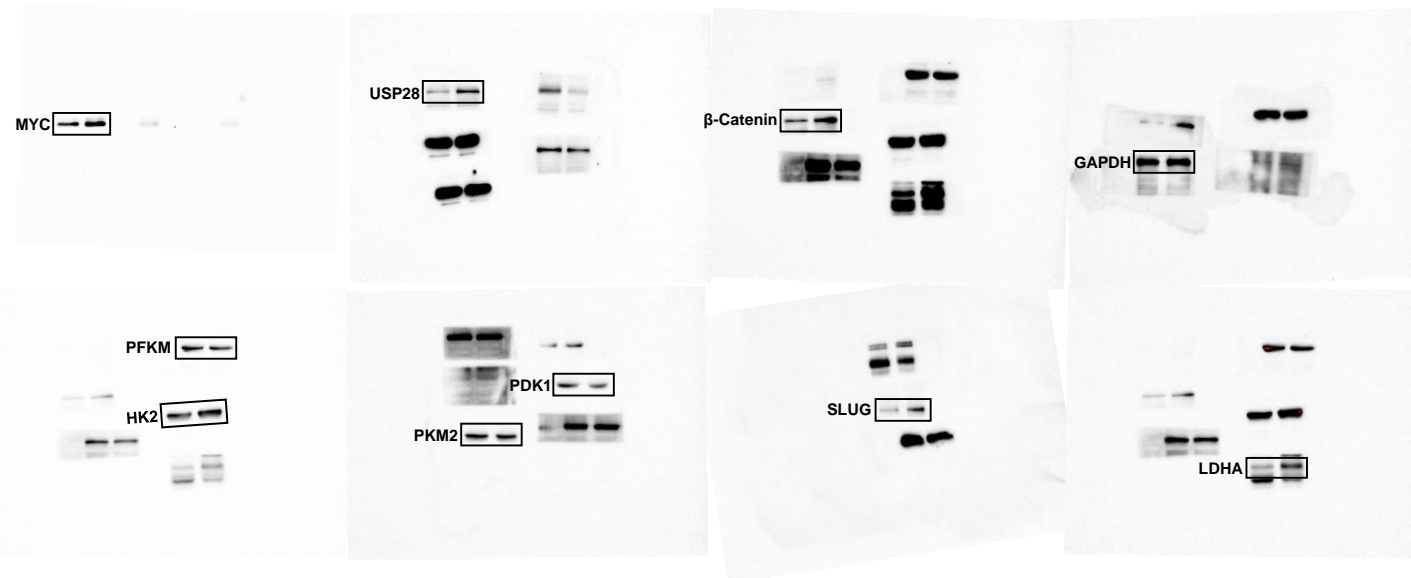
Full unedited gel for Figure 3F



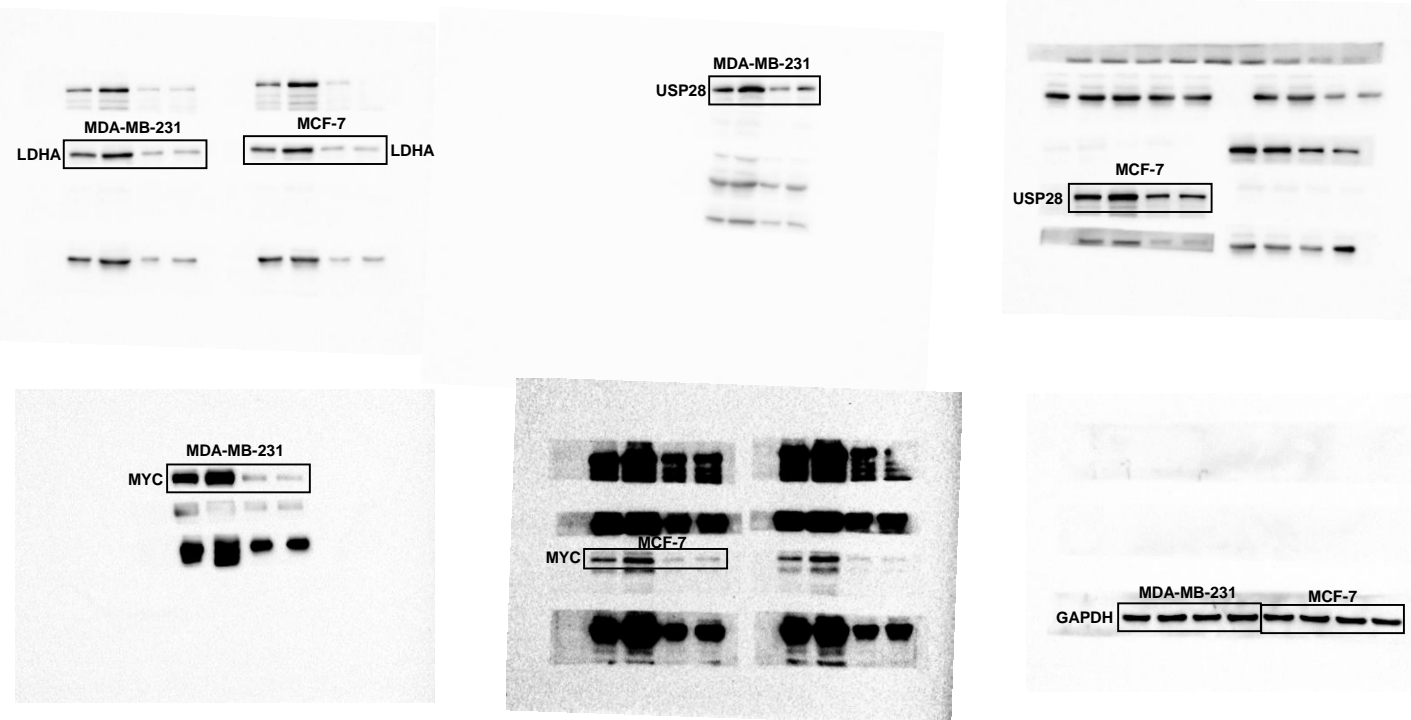
Full unedited gel for Figure 3H



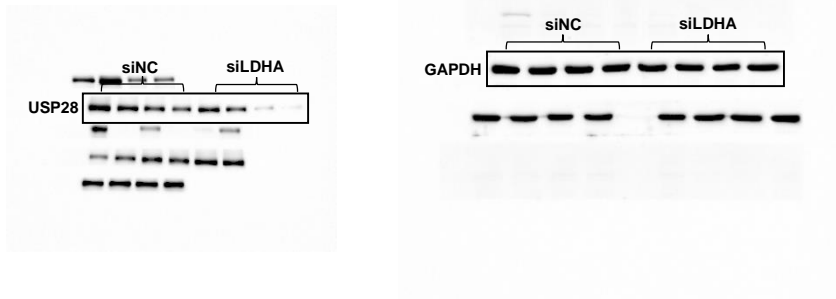
Full unedited gel for Figure 4D



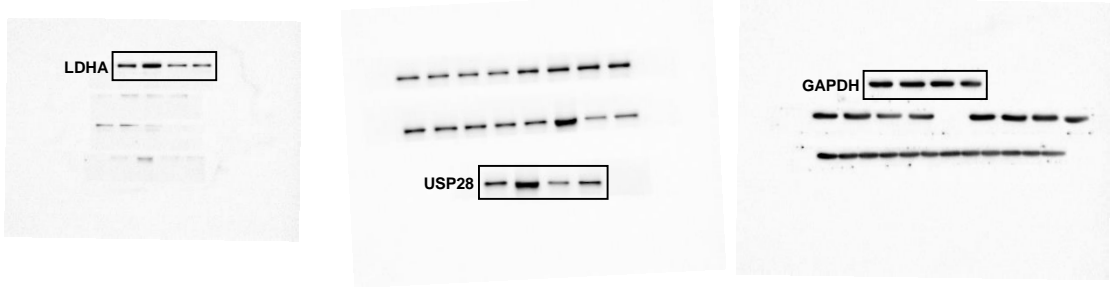
Full unedited gel for Figure 4E



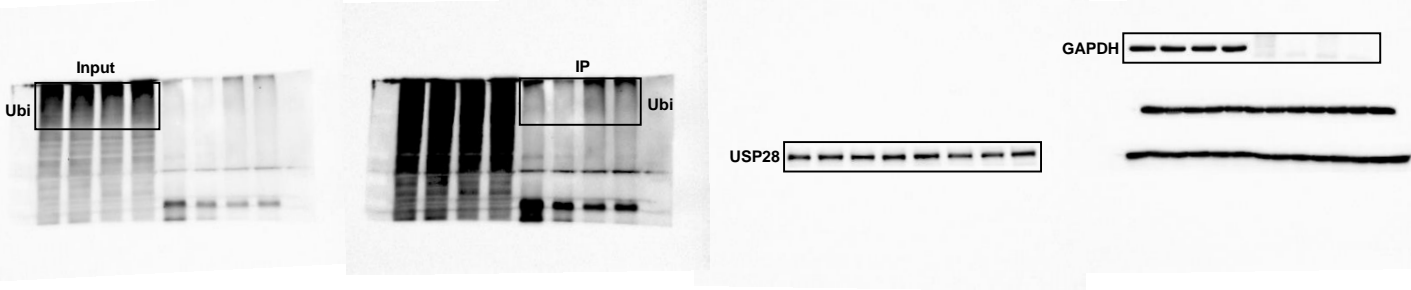
Full unedited gel for Figure 5A



Full unedited gel for Figure 5B



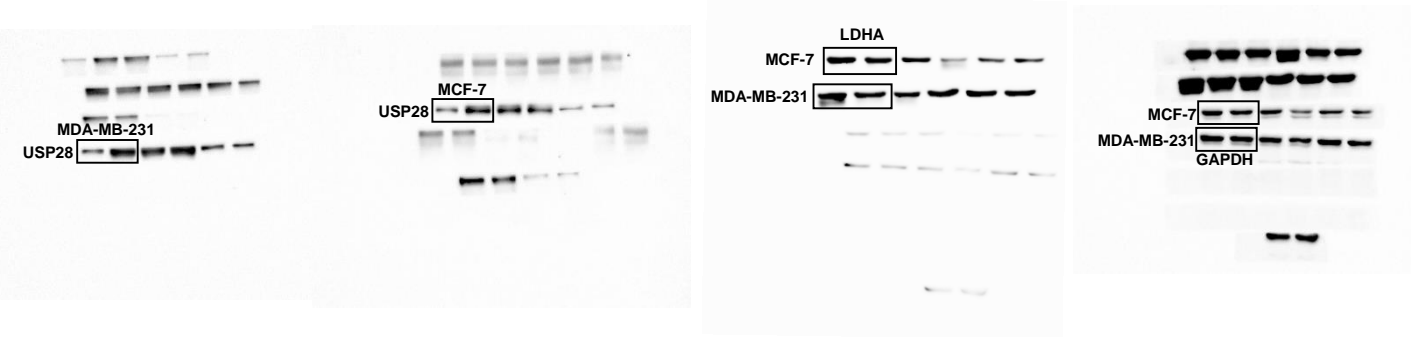
Full unedited gel for Figure 5C



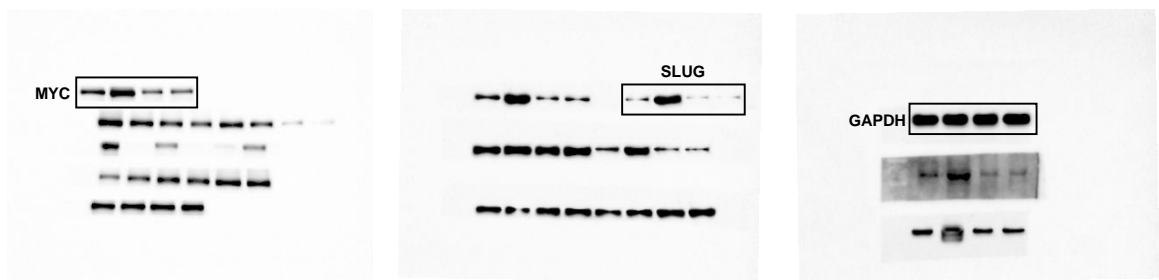
Full unedited gel for Figure 5D



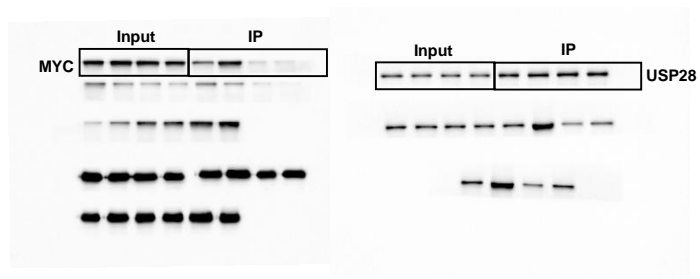
Full unedited gel for Figure 5E



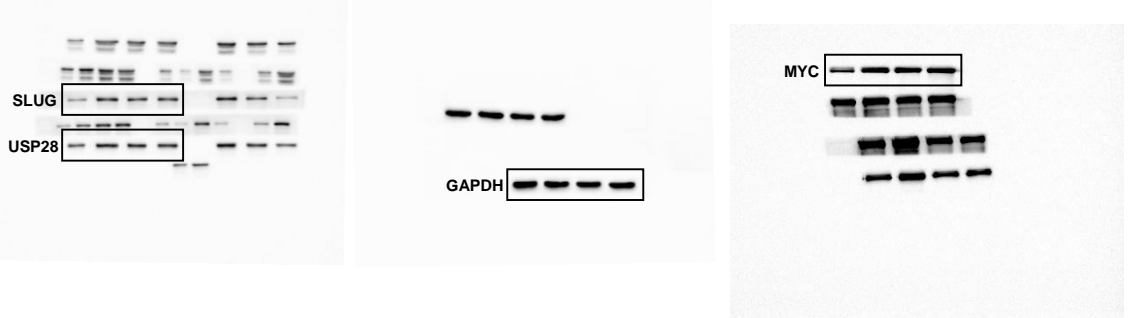
Full unedited gel for Figure 5F



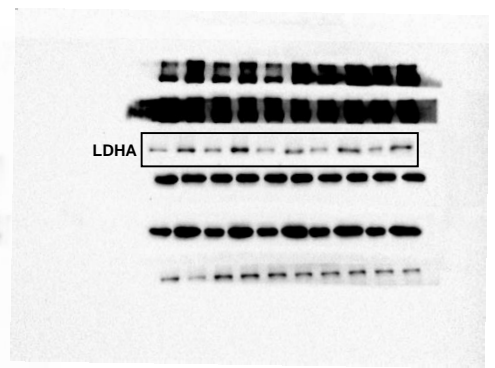
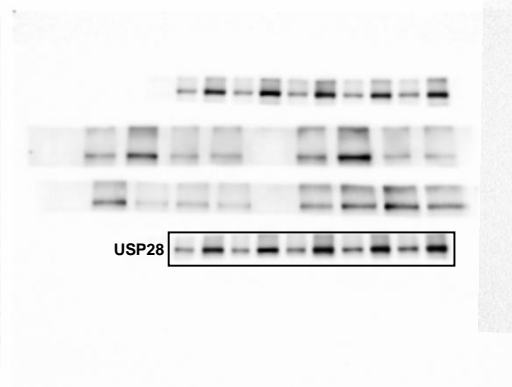
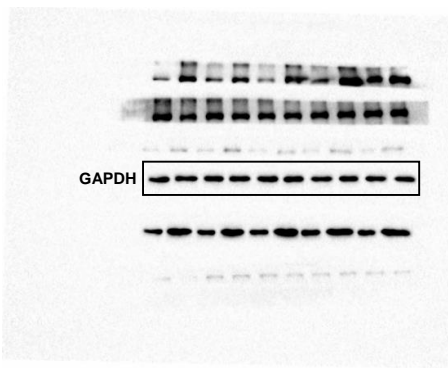
Full unedited gel for Figure 5G



Full unedited gel for Figure 5H

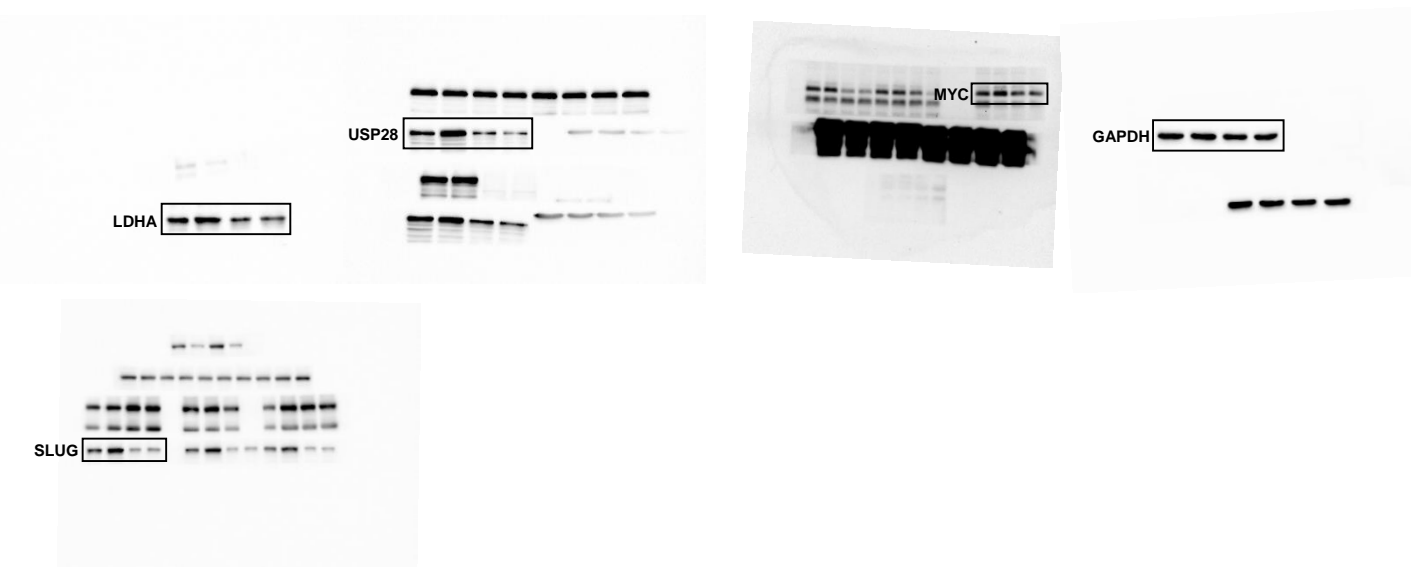


Full unedited gel for Figure 6B

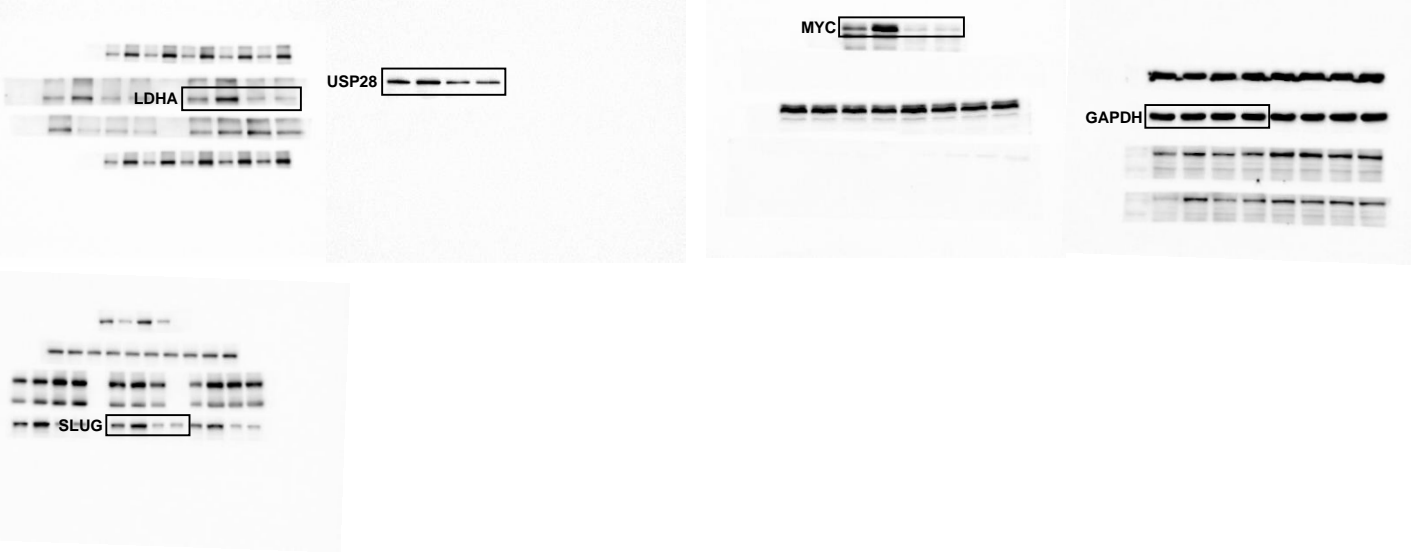


Full unedited gel for Figure 7C

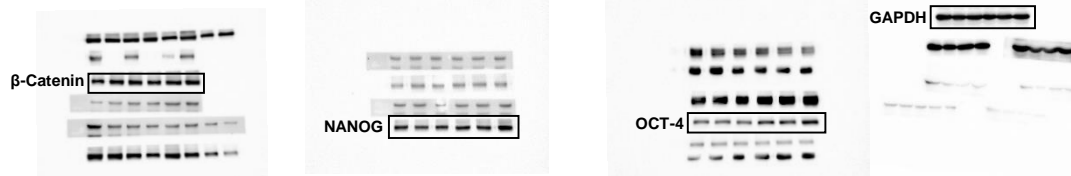
MDA-MB-231



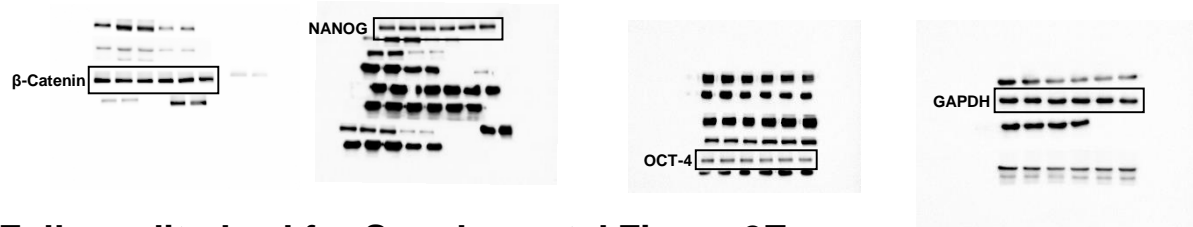
MCF-7



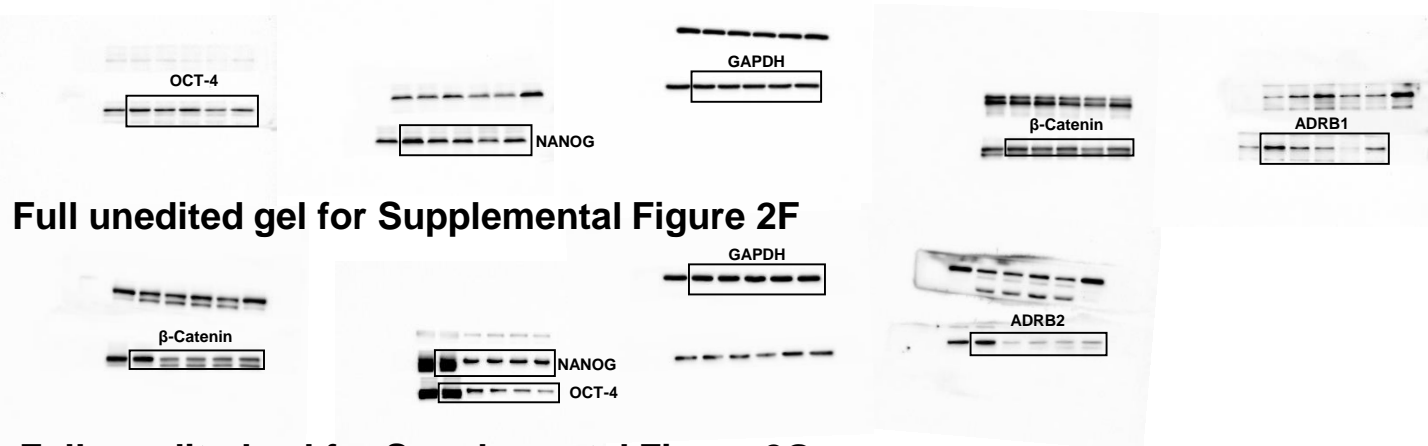
Full unedited gel for Supplemental Figure 2C



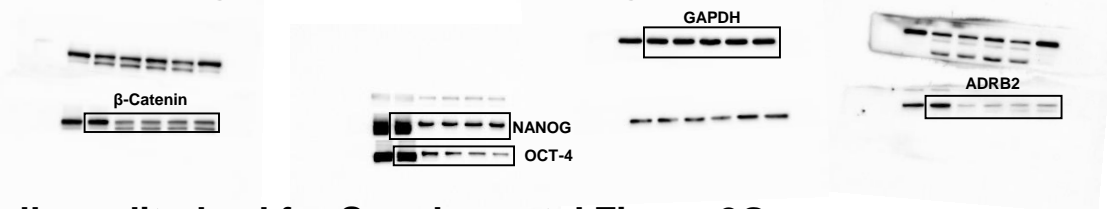
Full unedited gel for Supplemental Figure 2D



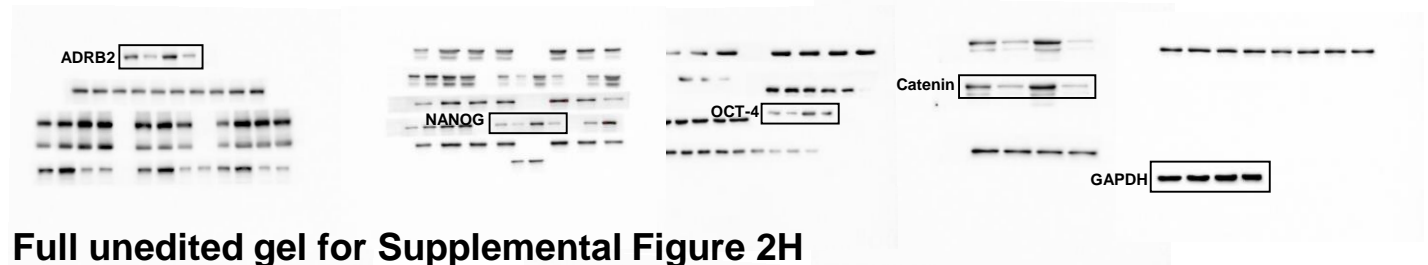
Full unedited gel for Supplemental Figure 2E



Full unedited gel for Supplemental Figure 2F



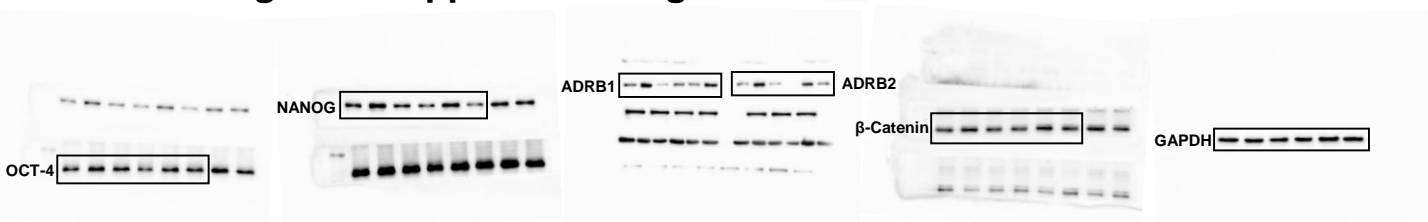
Full unedited gel for Supplemental Figure 2G



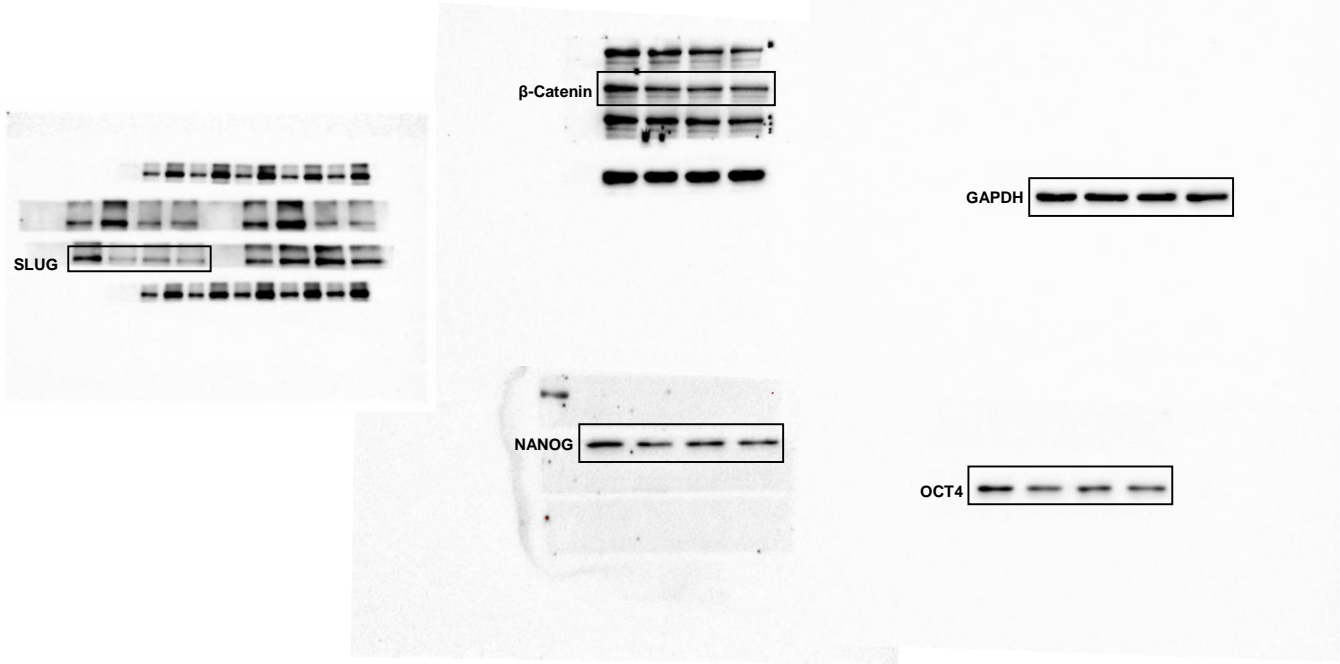
Full unedited gel for Supplemental Figure 2H



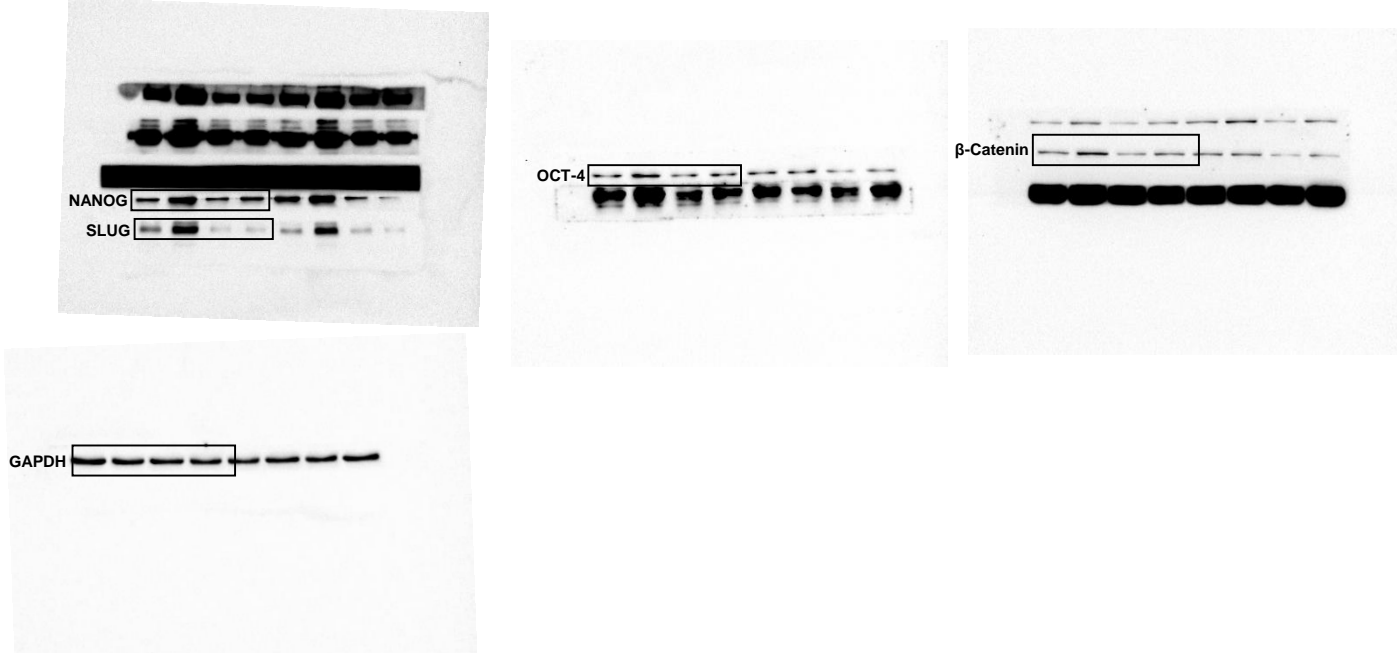
Full unedited gel for Supplemental Figure 2I



Full unedited gel for Supplemental Figure 3B



Full unedited gel for Supplemental Figure 3D

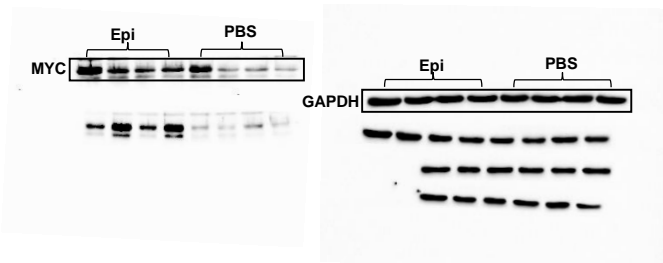


Full unedited gel for Supplemental Figure 3H



Full unedited gel for Supplemental Figure 4B

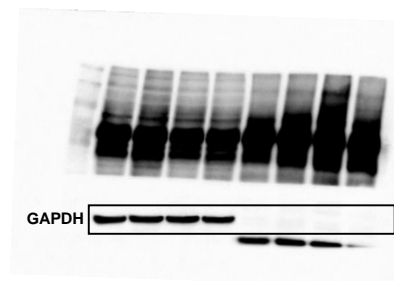
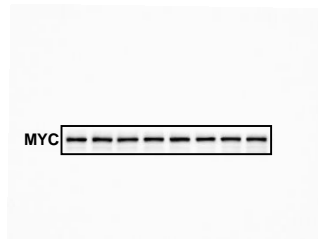
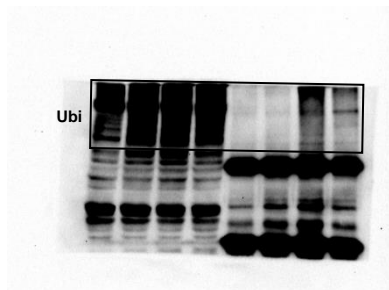
MDA-MB-231



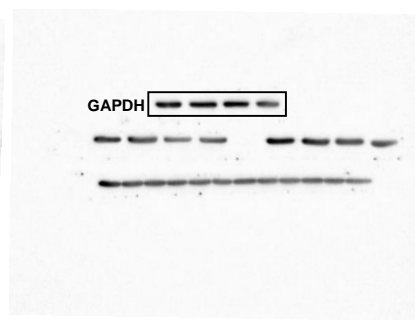
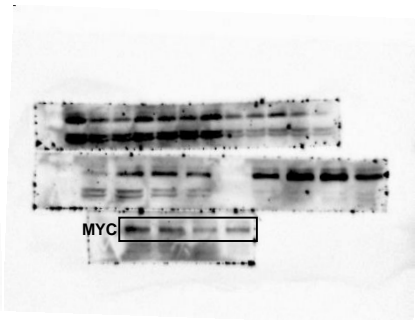
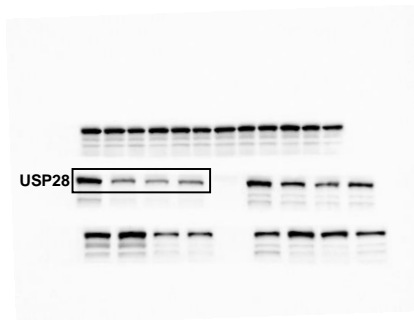
MCF-7



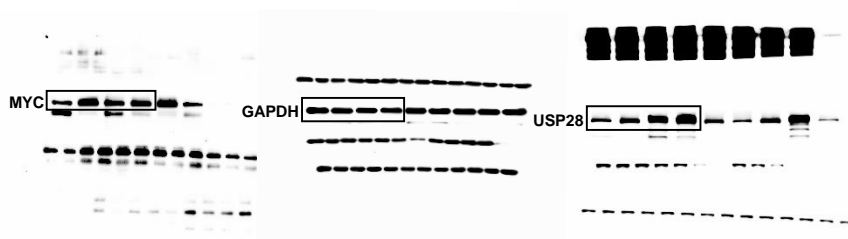
Full unedited gel for Supplemental Figure 4C



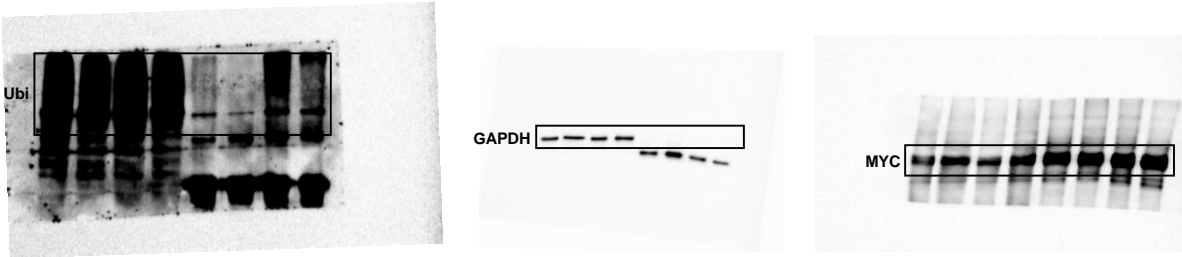
Full unedited gel for Supplemental Figure 4D



Full unedited gel for Supplemental Figure 4E



Full unedited gel for Supplemental Figure 4F



Full unedited gel for Supplemental Figure 4G



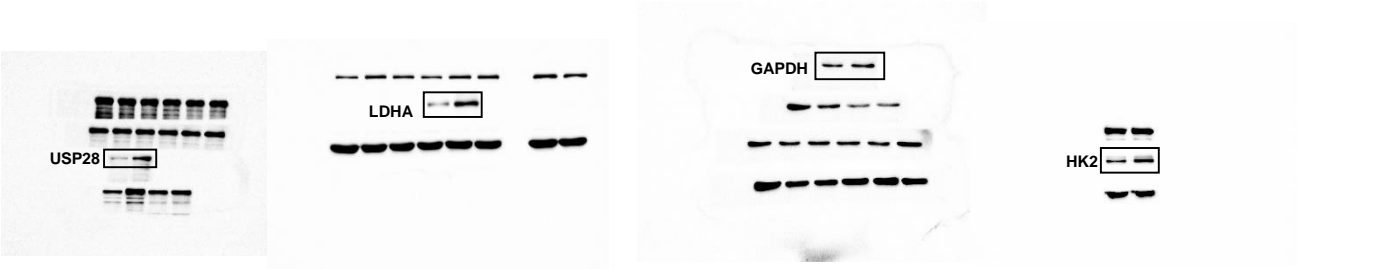
Full unedited gel for Supplemental Figure 4J



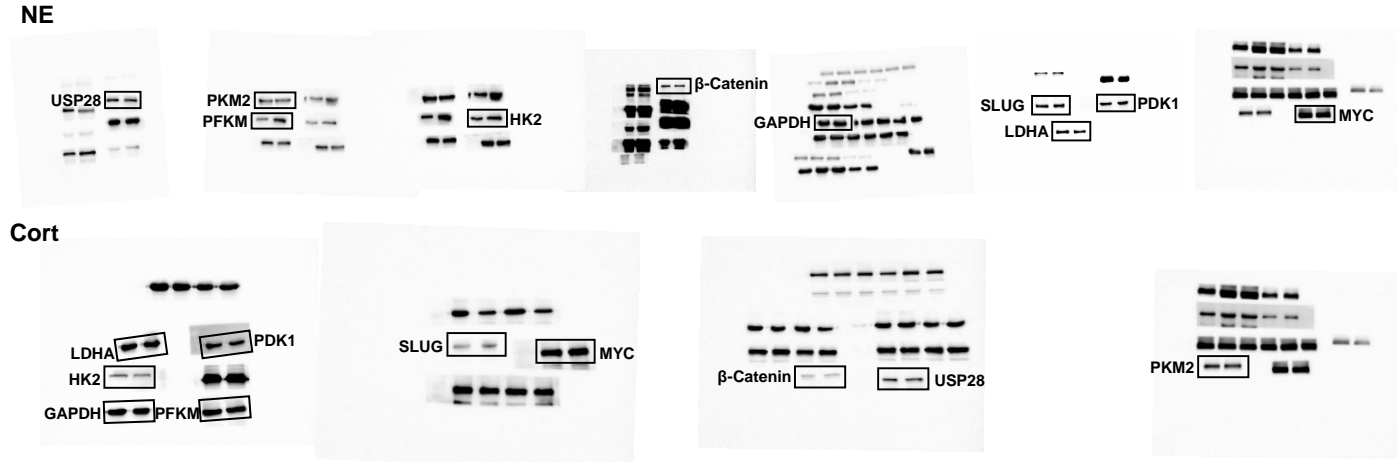
Full unedited gel for Supplemental Figure 4K



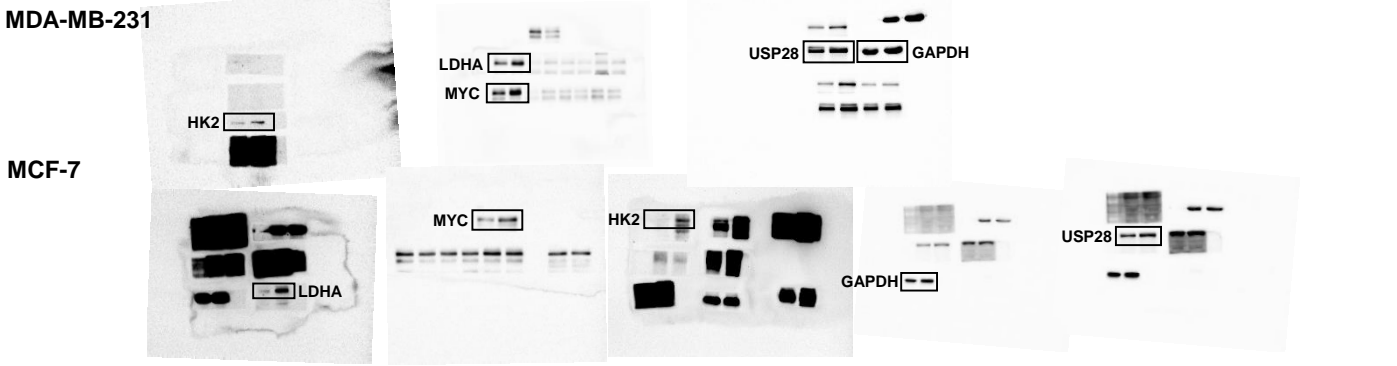
Full unedited gel for Supplemental Figure 5C



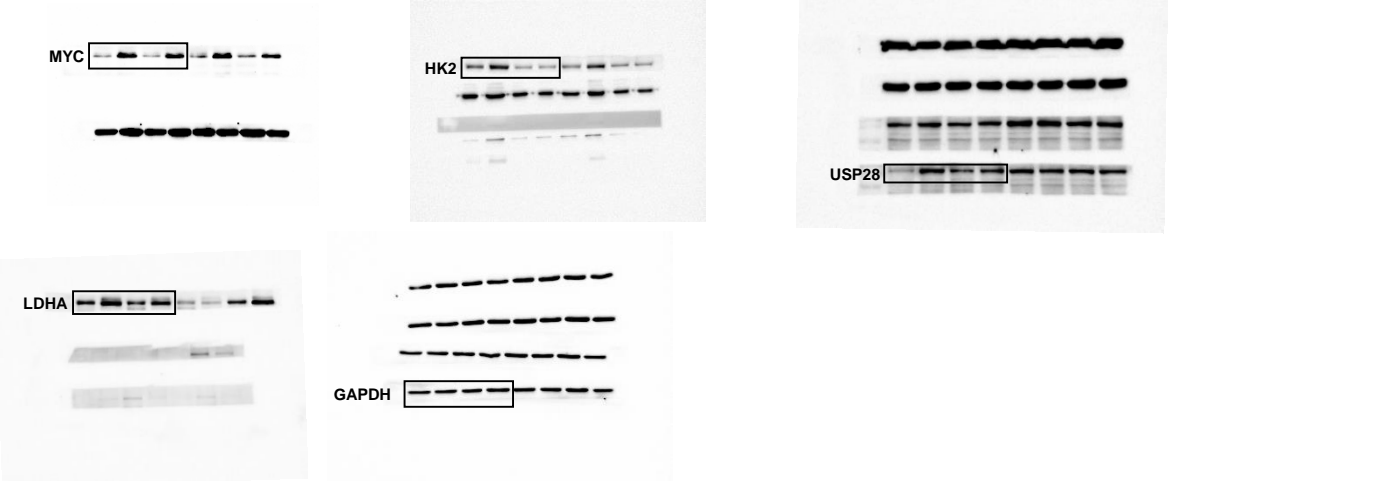
Full unedited gel for Supplemental Figure 5D



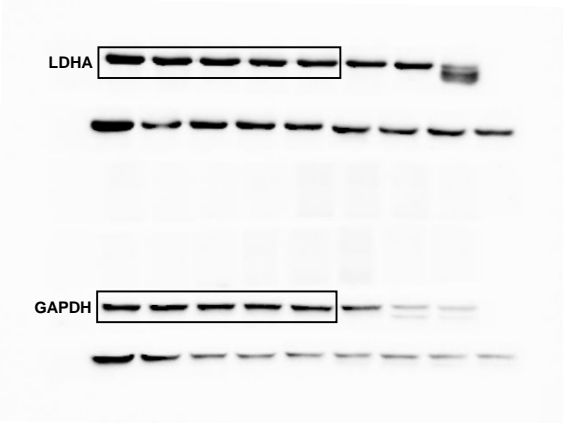
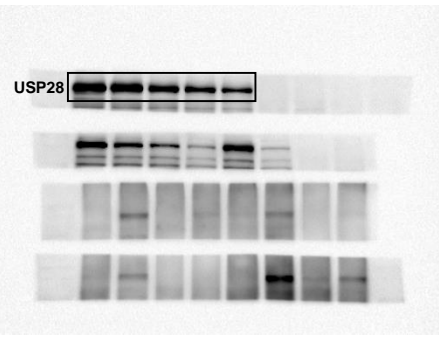
Full unedited gel for Supplemental Figure 5E



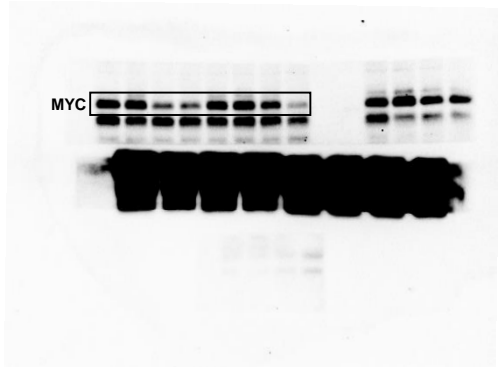
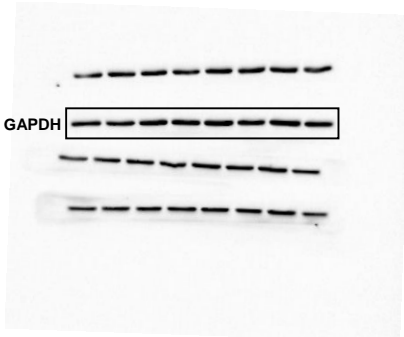
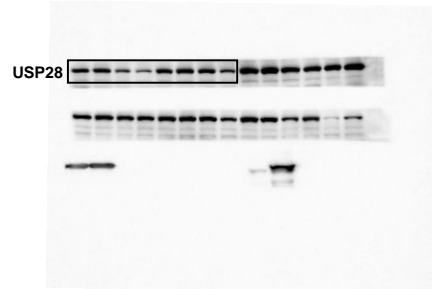
Full unedited gel for Supplemental Figure 5F



Full unedited gel for Supplemental Figure 6B



Full unedited gel for Supplemental Figure 6C



Full unedited gel for Supplemental Figure 6D

